2023 Salmon Methodology Review Material

Table of Contents

Methodology Review Progress Update: FRAM Base Period Documentation

Presented by: Derek Dapp and Ty Garber
Work conducted by the Salmon Modeling and Analytical Workgroup (SMAWG) and Salmon Model Evaluation Workgroup (MEW)

Progress since the last methodology review:

Since the last methodology review, we have focused on documenting the calibration process used to develop the Chinook base period. This information is now available under the "Base Period" tab, in the Chinook section, on the FRAM documentation website (see here). The base period documentation was designed to seamlessly integrate with the existing web-based FRAM documentation. It is written in R Markdown and contains the same user-friendly features, such as hyperlinks to referenced information, real-time content updates, easy navigation through table of content, etc. The code can be downloaded from GitHub.

The calibration process uses coded wire tag recoveries that have been processed in CAS and FRAMBuilder (additional details available here) to estimate base period parameters used in FRAM such as base period exploitation rates, base period cohort sizes, maturation rates, adult equivalent rates, and fishery model stock proportions. These base period parameters are then subsequently used in conjunction with annual input data in FRAM pre- and post-season runs to determine fishery-stock compositions, cohort sizes, and stock exploitation rates.

The following sections have been added to the documentation that describe the calibration process:

- An overview of calibration processes.
- Summaries of the extensive data preparation, decisions, and methodologies requiring updating before the actual calibration can commence, including several sections on the history of why decisions were made during base period construction such as whether to build the base period using CWTs from just marked fish or all CWTs (marked + unmarked), why the base period years were chosen, how new applications were developed, and how surrogate fisheries were implemented.
- Detailed descriptions of methods employed to handle sparse or missing CWT recoveries.
- Analyses of CWT recovery patterns.
- A description of main calibration procedures and calibration equations.
    - A description of variables and notations used in the calibration process.
    - A description of CWT expansion calculations.
    - A description of how fishery model stock proportions are determined.
    - An overview of how the calibration program estimates the total number of sublegal encounters and non-retention mortalities.
    - A summary of the cohort reconstruction process in the calibration program.
    - A description of growth function calculations.
    - Sections on calculating key outputs, including exploitation rates, maturation rates, and adult equivalent rates.
    - A description of out-of-base procedures needed to incorporate CWTs from out-of-base years for stocks with insufficient recoveries during base period years (2008-2013).

- Several sections that describe the input data used in the calibration program such as escapements, fisheries, fishery scalers, growth functions, incidental mortality, minimum size limits, model stock proportions, natural mortality, stocks, terminal fishery flags, and time steps.
- Several sections that define the output data from the calibration program, such as base period exploitation rates, fishery model stock proportions, maturation rates, sublegal encounter rates, and base period cohort sizes.
- Descriptions of FRAMBuilder and calibration programs with sections on prerequisites, conducting runs, code descriptions, transferring output, and specific instructions for producing a new base period.
- An appendix providing all the tables used in the calibration database.
- A glossary of key terms used in the calibration process.

Next steps:

Work on the FRAM documentation is on-going and there are several sections that the team would like to prioritize future work on for the next methodology review. These prospective sections are detailed below:

- Estimating the Stock Composition of Sublegal Encounters in the Calibration Process: Landed catch mortalities in the calibration process are estimated using coded wire tags. Sublegal fish are not landed and do not have coded wire tags returned by sampling programs. Therefore, sublegal mortalities and stock composition are estimated through a process that combines Von Bertalanffy growth functions and coded wire tag returns to estimate sublegal mortalities by stock.
- Canadian Catch Estimates in FRAM and the Calibration Process: Prior to the implementation of the Canadian iRec system (see here), Canadian catch estimates were not available in locations and periods where fishery sampling did not occur. Exclusion of these catch estimates had potential to bias FRAM exploitation rates in Canadian fisheries low. We collaborated with (Fisheries and Oceans Canada) DFO to produce unofficial catch estimates in spatio-temporal periods lacking fishery sampling. Documentation of this process will be important for understanding how inputs were developed as these inputs deviate from official catch estimates produced by DFO.
- Coded Wire Tag Inputs in the Calibration Process: While there is section dedicated to FRAMBuilder (the process that converts raw coded wire tags to the format needed by the calibration program) on the current documentation site and there has been progress made over the past year on describing special processing cases needed between FRAMBuilder and the calibration program (in the "Preparation" section of the calibration program documentation), there is additional processing of coded wire tags in the calibration program that could be described.
- Catch, Non-Retention, and Target Encounter Rate Inputs in the Calibration Process: Inputs used in the calibration program come from a wide variety of sources and it would be beneficial to document where these come from for reproducibility.
- Describing some exceptions for CWT handling, such as imputing freshwater sport recoveries and dealing with WCVI sport fisheries (inside vs. outside)

- Calibration Update Cycle: Updating the Chinook base period is a time consuming process that requires QA/QC from agencies along the West Coast and can potentially affect exploitation rate outputs used for management. The SMAWG has developed a calibration update cycle that should be included in the documentation.
- Fishery Profiles: While fishery names and FRAMIDs are described in Appendix 4, we aim to expand upon this section by describing the management areas that each fishery represents. Also, in situations where surrogate fishery or time steps were used, we anticipate documenting that in the fishery profiles section.
- Calibration Results: We are still discussing what might be the most appropriate material to put in this section, but we envision putting key outputs from the calibration program into a results section. Preliminarily, we might include figures that show output stock compositions in fisheries during the base period by time step, comparisons of new base period stock compositions with GSI data where available, and comparisons of how exploitation rates have changed for Puget Sound stocks across base period versions.
- Description of QAQC procedures.
- Description of outreach performed for new base period due to the many parties involved in the finalized product.

We appreciate any feedback that the SSC and STT might provide on documentation updates since the last methodology review or on future planned documentation updates.

Calculation of Chinook FRAM preseason fishery scalers for south of Cape Falcon fisheries

October 2023 Salmon Methodology Review

Jon Carey / NOAA Fisheries / jonathan.carey@noaa.gov

During the Pacific Fishery Management Council (Council) salmon fishery preseason planning process, the Chinook Fishery Regulation Assessment Model (FRAM) is used to estimate the expected impact from proposed fishery regulations on a variety of individual stocks of interest. Within FRAM, fisheries can be modeled using one of two input types:

- ***Quota:*** catch in the fishery set equal to a numeric value input by the user.
- ***Fishery Scaler:*** a scale factor relative to the fishing effort that occurred during the reference base period using a scaler value input by the user. The resulting catch is a function of the scaler input, the base period exploitation rates, and the stock abundances.

For fisheries that are quota-managed or have available estimates of projected total catch (all stocks), quota inputs are typically used. When fisheries are managed as seasons and have no estimates of projected total catch, a fishery scaler input can be used instead, as has traditionally been the case for Council managed fisheries that occur south of Cape Falcon (SOF). The status quo approach that has historically been used to derive fishery scaler inputs is to divide projected effort (an output of the Klamath Ocean Harvest Model) in the given year by the mean effort that occurred during the base period (currently 2007 – 2013; Table 1) for each fishery (f) and time step (ts).

$$Fishery\_Scaler_{f,ts} = \frac{Projected\_Effort_{f,ts}}{BP\_avg\_Effort_{f,ts}} \quad \text{(Eq 1)}$$

The expectation with this approach is that if the stock abundances in the model run year were equivalent to the average base period abundance, but the effort in a particular fishery were half of the base period effort, then the resulting catch in that fishery would be half of the base period catch. Similarly, if the effort in a fishery were equal to the average base period effort, but the abundances in the model run were double the base period abundance, then the fishery would be expected to catch approximately twice the base period catch.

We recently discovered that the status quo approach to calculating preseason fishery scalers is missing a key component. When applying this approach for a particular fishery/time period, a critical assumption is that the mean fishery scaler during the base period years is equal to or near 1.0. Beginning with the base period upgrade that occurred in 2017, this assumption no longer holds true in some instances (Table 2), thus, an additional step is required in deriving fishery scaler inputs for the SOF Council fisheries. Specifically, the ratio of projected effort to mean base period effort must also be multiplied by the mean fishery scaler that occurred over the base period years. A benefit in adding the mean fishery scaler term is that it allows a fishery scaler input to be calculated using a reference period (RP) that

differs from the base period years, as long as the year range used is consistent for both the mean effort and the mean fishery scaler.

$$Fishery\_Scaler_{f,ts} = \frac{Projected\_Effort_{f,ts}}{Avg\_Effort_{f,ts,RP}} * Avg\_FisheryScaler_{f,ts,RP} \quad \text{(Eq 2)}$$

The current Chinook FRAM base period spans fishing years 2007 – 2013. For two of these years (2008 – 2009) SOF fisheries were significantly restricted or closed. Given that, we conducted a retrospective assessment to evaluate whether excluding these years and instead using average effort and fishery scalers for a reference period of 2010 – 2013 would perform better than using base period years. For this assessment, we projected fishery catches for 2010 through 2018 using two sets of fishery scaler inputs for all SOF fishery and time step combinations based on observed effort from Appendix A of the Review of 2022 Ocean Salmon Fisheries. The first set of scalers were calculated using average effort and fishery scalers from the base period years (2007 – 2013), while the second set of scalers was calculated using a reference period of 2010 – 2013. Both were calculated using equation 2, which includes the adjustment for the average fishery scaler during the reference period.

Results of this assessment for each fishery on an annual basis are plotted in Figure 1 and performance metrics are presented for each reference period in Table 3. The resulting mean absolute percent errors suggest that using the 2010 – 2013 reference period would result in improved precision in catch projections for the KMZ troll and sport fisheries, but not the other Central Oregon and Southern California fisheries. The 2010 – 2013 reference period also resulted in mean raw errors for the KMZ fisheries that were closer to zero than those produced using 2007 – 2013. Based on these results, we recommend using the 2010 – 2013 reference period for the KMZ fisheries, but maintaining the 2007 – 2013 reference period for the Central Oregon and Southern California fisheries.

Using these recommended reference periods, we conducted an additional, similar retrospective assessment that compared performance of fishery scalers derived using equation 1 (status quo) and those derived using equation 2 (adjusted for average fishery scaler during the reference period). These results are presented in Figure 2 and Table 4, and confirm the need to include the average fishery scaler term when calculating the fishery scaler for a given fishery (i.e., use equation 2 instead of equation 1). When considering annual performance (summed across the three model time steps), the scalers derived using equation 2 performed better in all instances with the exception of two, which were essentially identical, regardless of the equation used.

Given these results, we recommend:

1. **Using equation 2 to calculate Chinook FRAM preseason fishery scaler inputs for Council fisheries south of Cape Falcon.**
2. **Using a reference period of 2007 – 2013 (base period years) for the Central Oregon and Southern California troll and sport fisheries, and a reference period of 2010 – 2013 for the KMZ troll and sport fisheries.**

The goal of these recommendations is to improve the ability of Chinook FRAM to project total catches in SOF Council fisheries. It is worth noting, though, that the implications of these recommendations on key Chinook FRAM output will be minimal, as Council fisheries that occur south of Cape Falcon generally have minimal impact on Chinook stocks that are assessed using FRAM. The one exception to this is the

Central Oregon Troll fishery, and the recommendations here will have little effect on the calculation of fishery scalers for this fishery, as we are not proposing to change the reference period and the average fishery scalers during the two time periods when the majority of catch occurs (May-Jun and Jul-Sep) are close to a value of 1.0 (Table 2).

Table 1. *Fishing effort for base period years by region, gear type, and time period for south of Cape Falcon fisheries as structured in Chinook FRAM. Effort units are in boat days for troll and angler trips for sport. Source: PFMC 2023. Review of 2022 Ocean Salmon Fisheries.*

		TROLL				SPORT			
Area	**Year**	**Oct-Dec**	**May-Jun**	**Jul-Sep**	**Oct-Dec**	**Oct-Dec**	**May-Jun**	**Jul-Sep**	**Oct-Dec**
Central OR[1/]	2007	1,370	1,955	1,719	406	5,577	9,072	53,202	2,381
	2008	406	0	37	60	2,381	3,253	16,368	2,348
	2009	60	0	634	60	2,348	4,144	60,184	2,009
	2010	60	2,002	1,324	473	2,009	3,823	32,244	1,145
	2011	473	1,968	429	983	1,145	3,398	30,362	1,659
	2012	983	2,370	1,765	1,830	1,659	5,400	36,123	2,895
	2013	1,830	1,905	4,010	2,000	2,895	4,881	49,024	4,437
	'07-'13 Avg	***740***	***1,457***	***1,417***	***830***	***2,573***	***4,853***	***39,644***	***2,411***
	'10-'13 Avg	***837***	***2,061***	***1,882***	***1,322***	***1,927***	***4,376***	***36,938***	***2,534***
KMZ[2/]	2007	184	146	611	59	3,081	8,569	19,723	3,263
	2008	59	0	0	51	3,263	712	3,018	1,065
	2009	51	0	0	0	1,065	268	11,022	0
	2010	0	43	66	72	0	1,436	6,473	2,270
	2011	72	120	295	75	2,270	5,218	14,234	1,757
	2012	75	141	505	54	1,757	13,133	33,404	3,666
	2013	54	452	851	62	3,666	14,274	32,115	3,547
	'07-'13 Avg	***71***	***129***	***333***	***53***	***2,157***	***6,230***	***17,141***	***2,224***
	'10-'13 Avg	***50***	***189***	***429***	***66***	***1,923***	***8,515***	***21,557***	***2,810***
Southern CA[3/]	2007	480	3,161	6,879	168	18,422	32,917	33,171	3,602
	2008	168	0	0	0	3,602	0	0	0
	2009	0	0	0	0	0	0	0	16,774
	2010	0	0	1,975	0	16,774	9,506	18,158	15,565
	2011	0	2,383	4,272	117	15,565	12,880	44,851	24,897
	2012	117	5,331	8,417	469	24,897	40,051	50,951	23,759
	2013	469	8,172	8,237	223	23,759	33,502	61,693	22,897
	'07-'13 Avg	***176***	***2,721***	***4,254***	***140***	***14,717***	***18,408***	***29,832***	***15,356***
	'10-'13 Avg	***147***	***3,972***	***5,725***	***202***	***20,249***	***23,985***	***43,913***	***21,780***

1/ Includes Tillamook, Newport, and Coos Bay

2/ Includes Brookings, Crescent City, and Eureka

3/ Includes Fort Bragg, San Francisco, and Monterey

Table 2. *Fishery scalers for base period years by region, gear type, and time period for south of Cape Falcon fisheries as structured in Chinook FRAM. Source: Chinook FRAM postseason runs based on calibration Round 7.1.1.*

		TROLL				SPORT			
Area	**Year**	**Oct-Dec**	**May-Jun**	**Jul-Sep**	**Oct-Dec**	**Oct-Dec**	**May-Jun**	**Jul-Sep**	**Oct-Dec**
Central OR	2007	0.6428	1.7664	2.2044	0.4908	3.6614	0.8689	0.4478	2.4626
	2008	0.1335	0.0000	0.0077	0.0049	1.0663	0.0222	0.0562	0.5390
	2009	0.0021	0.0000	0.0165	0.0102	0.5903	0.0201	0.0488	0.7382
	2010	0.0038	1.7106	0.5532	1.0650	0.2867	0.4606	0.2341	0.1744
	2011	0.7503	1.5578	0.1495	0.6513	0.1541	0.2758	0.2554	0.5429
	2012	0.4210	1.6624	1.1874	3.7281	0.2992	1.6585	0.5049	1.0589
	2013	2.4440	0.8622	2.5443	2.0367	0.5700	1.8706	0.8684	0.5316
	'07-'13 Avg	**0.6282**	**1.0799**	**0.9519**	**1.1410**	**0.9469**	**0.7395**	**0.3451**	**0.8639**
	'10-'13 Avg	***0.9048***	***1.4483***	***1.1086***	***1.8703***	***0.3275***	***1.0664***	***0.4657***	***0.5770***
KMZ	2007	--	0.8073	9.5644	--	--	2.8338	4.2333	--
	2008	--	0.0000	0.3388	--	--	0.0000	0.0946	--
	2009	--	0.0000	0.0000	--	--	0.0000	0.4053	--
	2010	--	0.2873	0.4858	--	--	0.0658	0.2187	--
	2011	--	0.9990	1.5414	--	--	0.5192	1.2617	--
	2012	--	1.1814	2.0180	--	--	1.6961	1.7058	--
	2013	--	3.2767	1.7967	--	--	1.3298	1.3184	--
	'07-'13 Avg	**--**	**0.9360**	**2.2493**	**--**	**--**	**0.9207**	**1.3197**	**--**
	'10-'13 Avg	***--***	***1.4361***	***1.4605***	***--***	***--***	***0.9027***	***1.1262***	***--***
Southern CA	2007	--	1.6114	2.6799	--	0.4426	1.2997	0.4487	0.1087
	2008	--	0.0000	0.0000	--	0.1224	0.0000	0.0000	0.0000
	2009	--	0.0000	0.0000	--	0.0000	0.0000	0.0000	1.2951
	2010	--	0.0000	0.4432	--	0.3898	0.2235	0.2155	0.3859
	2011	--	0.6184	1.2533	--	0.3442	0.2526	0.8712	1.2393
	2012	--	1.1338	1.1902	--	0.4378	0.5765	0.3883	0.3357
	2013	--	1.7630	0.9990	--	0.2963	0.4566	0.3678	0.2811
	'07-'13 Avg	**--**	**0.7324**	**0.9379**	**--**	**0.2904**	**0.4013**	**0.3274**	**0.5208**
	'10-'13 Avg	***--***	***0.8788***	***0.9714***	***--***	***0.3670***	***0.3773***	***0.4607***	***0.5605***

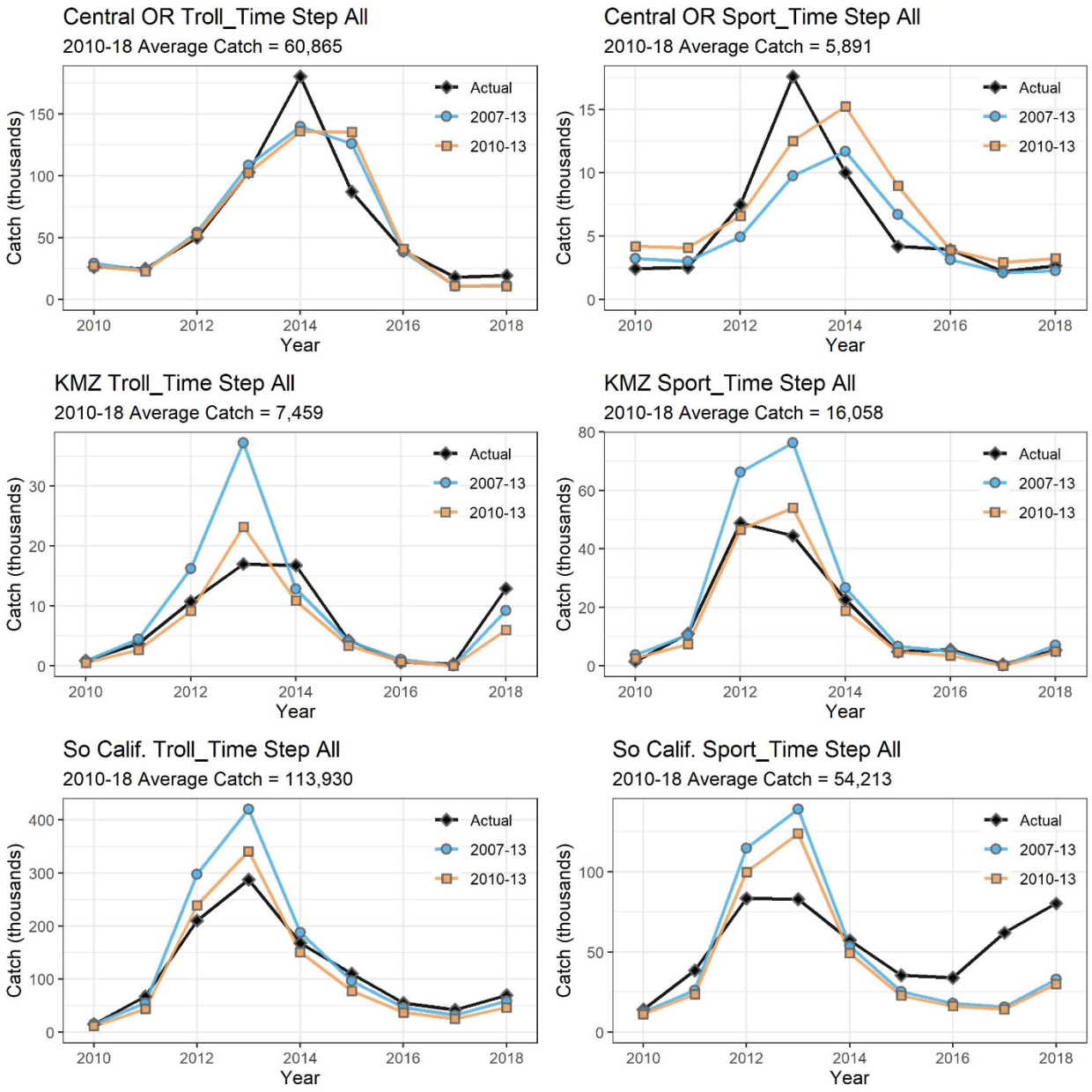

Figure 1. *Comparison of 2010 – 2018 actual (black line) annual catches (Oct-Sep management years) with projected catches that result from fishery scalers derived using equation 2 with actual effort and 2007 – 2013 (blue line) and 2010 – 2013 (orange line) reference periods.*

Table 3. *Comparison of mean raw error, mean percent error, and mean absolute percent error between catches projected using fishery scalers derived from 2007 – 2013 and 2010 – 2013 reference periods. Green shaded cells indicate better annual performance.*

	2007-13 Reference Period				2010-13 Reference Period			
	Oct-Apr	May-Jun	Jul-Sep	Total	Oct-Apr	May-Jun	Jul-Sep	Total
	Mean Raw Error							
Central OR Troll	5,056	-9	-5,658	-611	8,622	-1,107	-8,581	-1,066
Central OR Sport	328	-131	-882	-684	-105	163	897	956
KMZ Troll		-1,260	3,218	2,098		-1,132	-180	-1,185
KMZ Sport		1,582	4,974	6,380		-575	259	-252
Southern CA Troll		1,757	18,929	20,491		-8,699	1,887	-5,845
Southern CA Sport	-3	2,271	-7,876	-5,608	-742	-1,490	-8,509	-10,740
	Mean Percent Error							
Central OR Troll	378%	3%	-5%	-4%	509%	-2%	-16%	-6%
Central OR Sport	135%	2%	-5%	1%	8%	64%	38%	35%
KMZ Troll		-9%	47%	12%		-4%	-24%	-26%
KMZ Sport		51%	27%	24%		9%	-12%	-13%
Southern CA Troll		-12%	14%	1%		-28%	-11%	-19%
Southern CA Sport	-11%	4%	-20%	-17%	-19%	-25%	-22%	-26%
	Mean Absolute Percent Error							
Central OR Troll	397%	16%	40%	20%	521%	15%	41%	21%
Central OR Sport	146%	38%	22%	28%	31%	76%	47%	44%
KMZ Troll		26%	73%	48%		26%	42%	39%
KMZ Sport		59%	52%	49%		38%	31%	32%
Southern CA Troll		26%	24%	21%		29%	23%	26%
Southern CA Sport	27%	40%	46%	40%	29%	33%	47%	41%

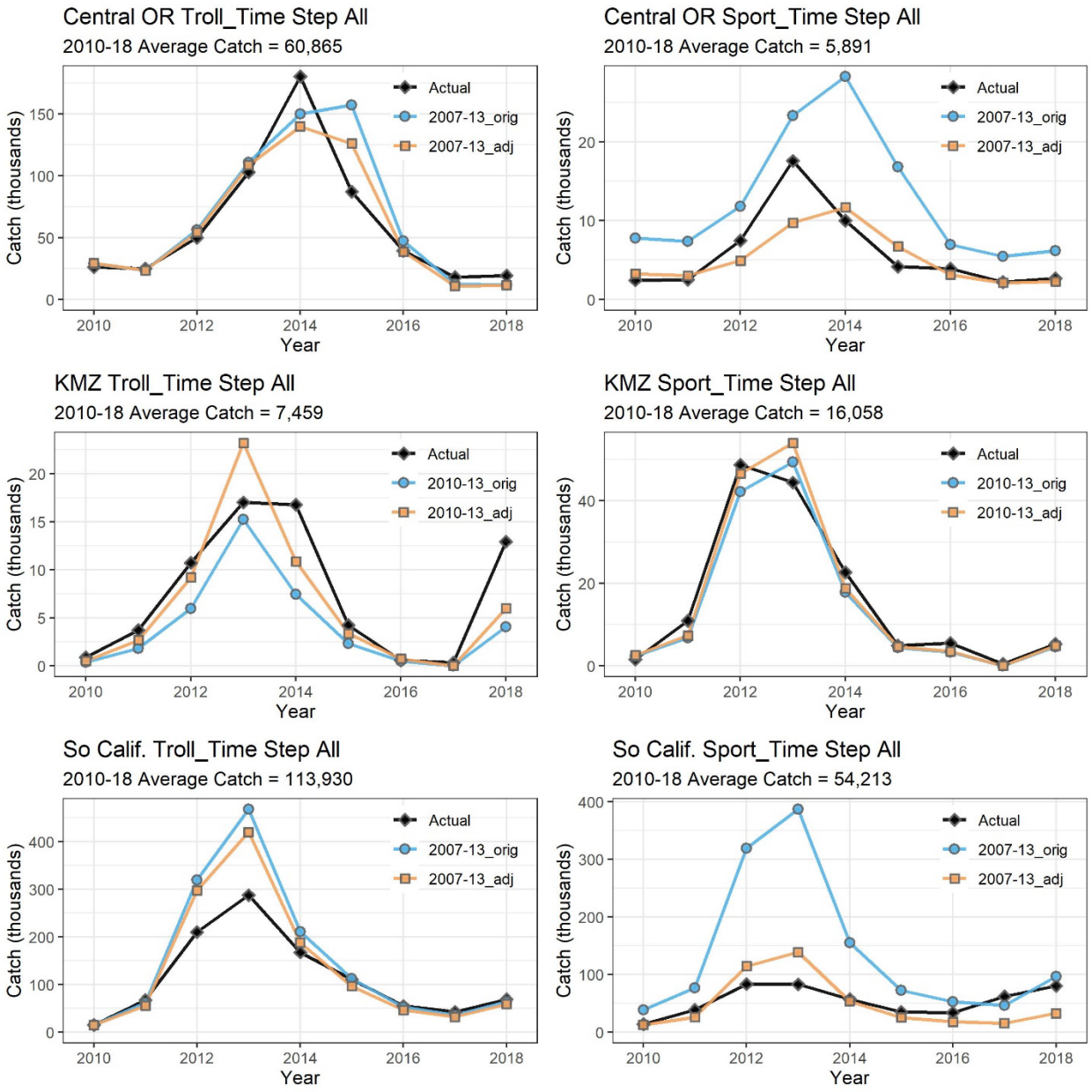

Figure 2. *Comparison of 2010 – 2018 actual (black line) annual catches (Oct-Sep management years) with projected catches that result from fishery scalers derived using equation 1 (blue line) and equation 2 (orange line). Central Oregon and Southern California fishery scalers were derived using a 2007 – 2013 reference period and KMZ fishery scalers were derived using a 2010 – 2013 reference period.*

Table 4. *Comparison of mean raw error, mean percent error, and mean absolute percent error between catches projected using fishery scalers derived from equation 1 (status quo) and equation 2 (average scaler adjusted). Central Oregon and Southern California fishery scalers were derived using a 2007 – 2013 reference period and KMZ fishery scalers were derived using a 2010 – 2013 reference period. Green shaded cells indicate better annual performance.*

	Original Scaler Equation (Eq 1)				Adjusted Scaler Equation (Eq 2)			
	Oct-Apr	**May-Jun**	**Jul-Sep**	**Total**	**Oct-Apr**	**May-Jun**	**Jul-Sep**	**Total**
	Mean Raw Error							
Central OR Troll	12,743	-1,713	-5,472	5,558	5,056	-9	-5,658	-611
Central OR Sport	373	38	6,376	6,788	328	-131	-882	-684
KMZ Troll	0	-1,815	-1,457	-3,272	0	-1,006	-180	-1,185
KMZ Sport	0	-75	-1,433	-1,507	0	-511	259	-252
Southern CA Troll	0	18,929	16,030	34,959	0	1,562	18,929	20,491
Southern CA Sport	22,158	21,582	40,284	84,024	-3	2,271	-7,876	-5,608
	Mean Percent Error							
Central OR Troll	661%	-5%	-3%	4%	378%	3%	-5%	-4%
Central OR Sport	148%	38%	173%	149%	135%	2%	-5%	1%
KMZ Troll		-34%	-50%	-50%		-4%	-24%	-26%
KMZ Sport		19%	-25%	-19%		9%	-12%	-13%
Southern CA Troll		17%	12%	12%		-12%	14%	1%
Southern CA Sport	205%	152%	130%	138%	-11%	4%	-20%	-17%
	Mean Absolute Percent Error							
Central OR Troll	664%	16%	41%	25%	397%	16%	40%	20%
Central OR Sport	158%	58%	173%	149%	146%	38%	22%	28%
KMZ Troll		38%	51%	50%		26%	42%	39%
KMZ Sport		41%	34%	33%		38%	31%	32%
Southern CA Troll		35%	21%	20%		26%	24%	21%
Southern CA Sport	205%	156%	138%	144%	27%	40%	46%	40%

A re-evaluation of preseason abundance forecasts for Sacramento River winter Chinook salmon

Tanya Rogers
Michael O'Farrell

Fisheries Ecology Division
Southwest Fisheries Science Center
National Marine Fisheries Service
National Oceanic and Atmospheric Administration
Santa Cruz, CA

September 22, 2023

Introduction

The Sacramento River winter Chinook salmon (SRWC) Evolutionarily Significant Unit (ESU) is listed as endangered under the United States Endangered Species Act, and is exposed to ocean salmon fisheries occurring along the U.S. west coast, primarily off central California.

Fishery management measures aimed at reducing impacts to SRWC have been in place since 1989 (O'Farrell & Satterthwaite 2015). Beginning in 2012, harvest-related impacts on age-3 SRWC have been managed using a harvest control rule that specified maximum allowable age-3 impact rates south of Point Arena, California, based on a forecast of abundance. Initially, the "forecast" of abundance was the most recent three year geometric mean of the number of spawners. However, it was clear that such a retrospective measure of abundance would be unable to respond to abrupt changes in abundance brought about by, for example, drought conditions. In recognition of this, the Pacific Fishery Management Council (PFMC) formed an ad hoc Workgroup in 2016 to explore alternative, forward looking control rules for SRWC. In 2018, a new SRWC harvest control rule was adopted by the PFMC. The form of the control rule differed from the previously adopted control rule, and it also required a forecast of abundance for implementation. A brief description of these changes to SRWC assessment and management can be found in PFMC (2018), Appendix A and Appendix D.

Many common salmon abundance forecasting approaches (e.g., sibling regressions) are not feasible for SRWC. Age-2 (jack) returns return estimates are not available when abundance forecasts are needed for PFMC fishery planning. While SRWC return to the river in winter, they delay spawning until summer and estimates of jack returns are made in the fall. The age-3 portion of the cohort that remained in the ocean (rather than returning to the river at age-2) has already encountered ocean fisheries when the age-2 escapement estimates are first available. Because of this, alternative forecasting methods for SRWC needed to be developed. In 2016, alternative forecast methods were presented to the PFMC's Scientific

and Statistical Committee (O'Farrell et al. 2016). Three forecast scenarios were presented: (1) *Base*, (2) *ETF*, and (3) *No JPI*. Each of these scenarios utilized inputs derived from a population dynamics model (Winship et al. 2014) to forecast SRWC age-3 escapement absent fishing. Descriptions of the forecast scenarios can be found in section 4 of O'Farrell et al. (2016), but are also summarized in the Forecast Model Specification section that follows. The recommendation stated in O'Farrell et al. (2016) was to use the *Base* model for forecasting SRWC abundance, but to monitor the performance of the *ETF* model as data accumulated. The *Base* forecasting approach has been used to forecast SRWC abundance each year since 2018. However, the performance of the alternative forecasting approaches has not been routinely assessed.

In this report we evaluate the forecast performance for the *Base* and *ETF* forecast models for a more extended range of years than was possible in 2016. Due to the relatively poor predictive performance of these models, we also assessed the performance of alternative models not evaluated in O'Farrell et al. (2016).

Forecast Model Specification

Base model

The *Base* forecasting approach which has been used to forecast SRWC abundance since 2018 is described in O'Farrell et al. (2016), section 2. Fitted inputs are the number of natural-origin female spawners and the fry-equivalent Juvenile Production Index (JPI), which is the estimated river-origin SRWC-sized juveniles passing Red Bluff Diversion Dam (RBDD), standardized to the fry stage (Voss & Poytress 2022). This model also uses environmental temperature (DD12: degree days above 12°C from May 15–October 31 at Clear Creek Gage; Table 1) as a covariate for the egg-to-fry survival rate. Specifically, the egg-to-fry survival rate is modeled using a Beverton-Holt function, and the parameter determining maximum survival rate is a function of the temperature covariate.

It is possible that in some years an empirical estimate of the JPI will not be available. In the absence of a JPI estimate, a model-based estimate, derived from the egg-to-fry relationship was developed. This is referred to as the *no JPI* forecasting approach. A diagram showing the steps in the forecast process for the *Base* and *no JPI* forecast models can be found in Figure 2 of O'Farrell et al. (2016). The performance of the *no JPI* model was not reevaluated in this study.

ETF model

The *ETF* forecasting approach is identical to the *Base* forecasting approach, with one exception: the juvenile survival rate (the survival rate from fry to age-2 in the ocean) is modeled as a function of the empirical egg-to-fry survival rate (Table 1). The empirical ETF survival rate is calculated from the JPI,

the number of eggs per female, and number of spawning females. As in O'Farrell et al. (2016), we use the ETF survival rates from Poytress (2016) for brood years 1996-1999, and the model-based estimates reported in O'Farrell et al. (2016) for years 2000-2001. The ETF survival rates used in O'Farrell et al. (2016) for brood years 2002-2015 were computed using the number of natural-origin females spawning in the river. However, that calculation did not account for hatchery-origin females spawning in the river, which contribute to the JPI. Thus, for brood years 2002-2020, we used updated ETF survival rates from Voss & Poytress (2022) and a final but unpublished value for brood year 2021 (Poytress, pers. comm.), which are based on the total number of females spawning in the river (natural and hatchery origin). Given these updates, along with other minor updates to the population dynamics model inputs, the return year 2012-2015 forecasts from the *ETF* model differ quite a bit from those reported in O'Farrell et al. (2016). The *Base* model forecasts differ by only a small amount.

Gaussian process (*GP*) model

The *GP* model relates several covariates (the empirical ETF survival rate, temperature covariate, total number of spawning females in the river, number of hatchery pre-smolts released; Table 1) directly to postseason escapement estimates using a nonparametric function approximator (specifically, a separable length scale Bayesian Gaussian process model). The rationale is that postseason escapement will be some function of these empirically measurable covariates, plus process noise. The *Base* and *ETF* models relate the covariates to the target in a complex and indirect way, requiring many assumptions (potentially incorrect) about population dynamics, functional forms, and how the covariates relate to population processes. The nonparametric approach, on the other hand, fits a flexible function directly relating the covariates to the target. This approach makes few assumptions about the shape of this relationship, which is informed only by the data. We explored whether this simpler, data-driven approach might produce better forecasts.

There are many different types of flexible function approximators. Some examples are splines, generalized additive models (GAMs), random forests, and neural networks. We chose to use Bayesian Gaussian process regression because it is relatively conservative (does not tend to over-extrapolate), allows for arbitrary interactions among predictors (does not assume additivity), can be fit with relatively little data because of the existence of priors, and allows the use of priors to prevent overfitting. The posterior mode can also be found quickly using gradient descent methods without the use of MCMC. GPs are widely used for spatial interpolation (i.e. kriging), but GPs can be used to flexibly fit any predictor surface in any number of dimensions (Rasmussen & Williams 2006).

We specifically used the GP model formulation described in Munch et al. (2017) and implemented in the R package 'GPEDM' (Munch & Rogers 2022). The method uses a squared exponential covariance

function, separate inverse length scale hyperparameters for each predictor, and priors on the inverse length scale hyperparameters to prevent overfitting (known in the machine learning literature as automatic relevance determination, Neal 1996). The priors have a mode at 0, so that irrelevant predictors are effectively 'dropped' from the model, and are set such that the expected number of local extrema over the range of each predictor is 1, thus preventing overly wiggly functions unless sufficiently supported by the data. The posterior mode is obtained using the R-prop algorithm (Blum & Riedmiller 2013). For more details, see Munch et al. (2017). Although the package and methodology can be used for empirical dynamic modeling (EDM), which uses time lags of the target variable (or a mixture of time lags and covariates) as predictors, the model used here *does not* do this. We fit the GP just using covariates. Using time lags (EDM) has higher data requirements than are available for SRWC, and we found that time lags did not improve prediction of SRWC escapement beyond the available covariates, likely because of insufficient data. In the final model, the response variable was the postseason estimate of age-3 escapement absent fishing (log transformed, thus assuming lognormal error). Predictions were back-transformed for fit evaluations. Predictor variables were the empirical ETF survival rate, temperature covariate (log(x+1) transformed), total number of females (natural + hatchery origin) spawning in the river (log transformed), and number of hatchery pre-smolts released (log transformed) for the brood year three years prior to the return year to be forecasted. We fit models using all combinations of these predictors and selected that with the best performance using leave-future-out cross validation.

Assessment of Forecast Performance

Forecasts of the SRWC age-3 escapement absent fishing ($\hat{E}_3^0$) made with the *Base*, *ETF*, and *GP* models were compared to postseason estimates (E_3^0) using leave-future-out cross validation for return years 2012-2022. Predictions were also made and compared for return years 2023-2024, although these were not used to evaluate performance since a postseason estimate was not available at the time of analysis.

Two methods were used to estimate E_3^0 (Table 2). The first method is identical to that used in O'Farrell et al. (2016)

$$E_{t,3}^0 = \frac{E_{t,a\geq 3} \times \bar{p}_3}{1 - i_{t-1,3}}$$

where $E_{t,a\geq 3}$ is the estimated escapement of SRWC adults (age-3 and older) in year *t*, $\bar{p}_3$is the average proportion of adult SRWC escapement that is age-3, and $i_{t-1,3}$ is the estimated age-3 impact rate. These values come from a cohort reconstruction model based on coded wire tag (CWT) data (O'Farrell et al. 2012). The second method is the same as the first, but year-specific estimates of p_3 were used instead of $\bar{p}_3$. Performance of each forecast model was evaluated with respect to E_3^0 calculated using the average (as

opposed to year-specific) proportion of adult escapement that is age-3. Results were very similar using year-specific values, since the average and year-specific E_3^0 values were very similar in most years.

Forecast performance of each method was evaluated using several different metrics. As in O'Farrell et al. (2016), we compute mean error (ME, reflecting bias), and root mean squared error (RMSE, reflecting accuracy). We also calculated mean percent error (MPE, reflecting bias), mean absolute percent error (MAPE, representing accuracy), and median log accuracy ratio (MLAR) (Satterthwaite & Shelton 2023). The MLAR (Morley et al. 2018) is equally sensitive to proportional over- vs. under-forecasts, with positive values indicating over-forecasting. Additionally, we calculated R^2, the proportion of variance explained, as

$$R^2 = 1 - \Sigma_t(E_{t,3}^0 - \hat{E}_{t,3}^0)^2 / \Sigma_t(E_{t,3}^0 - \bar{E}_3^0)^2.$$

In out-of-sample forecasts, such as we are performing here, the R^2 value can be negative, indicating that predictions are biased and worse than the mean, $\bar{E}_3^0$. Finally, we calculated *r*, the Pearson correlation coefficient between the predicted and observed values, which reflects whether the forecasts follow the same trend, but does not account for bias.

Results

There were two best performing *GP* models, which we label *GP-1* and *GP-2* (Table 3). *GP-1* had two predictors: the temperature covariate and the number of spawners. *GP-2* had the same two predictors as *GP-1* plus the number of hatchery pre-smolts released. The models had similar RMSE, R^2, and *r* values. The *GP-1* model had lower MPE and MAPE, whereas the *GP-2* model had lower ME. In both models, the conditional effect of the temperature covariate was unimodal (Figure 1). Escapement was highest at low-mid temperatures and declined with increasing temperature. Escapement at the lowest temperature values was still relatively high, but slightly below the peak. This is consistent with plots of the raw data. In both models, escapement increased with the number of spawners, although this relationship was weaker than that of temperature (Figure 1). As the amount of training data increased, the effect of temperature remained fairly consistent, and the effect of spawners became weaker (Figure 1). In the *GP-2* model, the hatchery releases initially had no effect on escapement, but as the most recent years of training data were added, hatchery releases were found to have a positive effect on escapement (Figure 1).

When using E_3^0 based on year-specific (rather than average) estimates as the response variable, the *GP-1* model and a model with the same predictors plus empirical ETF had similar performance; however, the 3 predictor model produced some unrealistic conditional relationships with the predictors and was sensitive to starting values of the hyperparameters, so the *GP-1* model would be recommended. For this response variable, using natural-origin (as opposed to total) spawners also produced somewhat better fits.

The leave-future-out preseason forecasts from each model are presented in Table 2 and Figure 2. As was found previously, the *ETF* model produced less precise estimates than the *Base* model, particularly for return years 2012-2014, which had extremely large credible intervals. The model with the most accurate prediction varied from year to year, but the *GP* predictions tended to be closest most consistently (Figure 3). Over return years 2012-2022, the *Base* model median had the best fit statistics for ME and MLAR, but the *GP* models had the best values for RMSE, MAPE, R^2, and *r* (Table 4). Only the *GP* models had positive R^2 and *r* values. If we exclude the first 3 test years in which the *ETF* model substantially overestimates escapement and evaluate fit statistics just over return years 2015-2022, the *ETF* model median performs somewhat better, with lower RMSE and MAPE than the *Base* model median, and has a positive *r* value (Table 5). The *ETF* model predictions were closer to the postseason estimates than the *Base* model in 5 of the last 8 years of test data. However, the *GP* models still had the best ME, RMSE, R^2, and *r* values over this later time period. All models agreed that escapement in 2024 is going to be relatively low.

The empirical ETF survival rates were not well correlated with the juvenile survival rates obtained from the cohort reconstruction model (Figure 4). There were some years with high escapement and high juvenile survival rates that had moderate ETF survival rates. These tended to be years with favorable temperature conditions.

Discussion

We evaluated the relative performance of SRWC abundance forecasts for the status quo *Base* model, the *ETF* model, and *GP* models informed by a range of predictor variables. Forecast model performance was assessed using a leave-future-out cross validation approach, where accuracy and bias were assessed using a range of performance metrics.

The *ETF* model performed better than the *Base* model in the most recent years, but performance of both models in general was poor. Two *GP* models tended to produce the best performing forecasts. The *GP* models suggested that of the variables available, temperature during egg incubation and outmigration (DD12) was the most important and consistent driver in determining SRWC returns. The slight decline in returns at the lowest DD12 levels was unexpected, but consistent with the raw data. The declining influence of parental spawners and increasing influence of hatchery releases in the *GP* model in the most recent years (Figure 1) likely reflects the sustained increases in hatchery production beginning in brood year 2014 (noting that there have been less consistent spikes in hatchery releases occurring prior to brood year 2014).

The greater accuracy and precision of the *GP* model forecasts is likely because, in contrast to the *Base* and *ETF* models, the *GP* model is fit directly to the target, E_3^0, and is more flexible in how the

covariates relate to it. The population dynamics model is fit to only two data streams: the number of natural-origin female spawners and the JPI. In this case, $\hat{E}_3^0$ is a derived quantity based on the number of juveniles multiplied by the modeled average juvenile survival rate, fixed maturation rates, and a fixed adult survival rate (0.8). The ultimate value of E_3^0, which is based on the observed total number of spawners, the proportion of total spawners that is age-3, and exploitation rates from the cohort reconstruction model, is not part of the likelihood.

Forecasts made with the *GP* models have lower input data requirements than the *Base* or *ETF* models, and take significantly less time to run. The *Base* and *ETF* models require inputs from a cohort reconstruction and population dynamics model that are implemented annually. If either model is unable to be implemented (which could happen for a variety of reasons), the status quo forecasting procedure would need to be modified and/or forced to rely on outdated estimates from the models. In contrast, the *GP* models have inputs that come from very reliable data streams. Estimates of spawners are made each year, the number of hatchery SRWC released each year is enumerated, and the DD12 predictor is derived from gage data.

Recommendation

Adoption of the *GP-2* model for future SRWC abundance forecasts is recommended. This model has similar forecast performance to the *GP-1* model, with slightly better performance in recent years due to the inclusion of data on hatchery releases. Inclusion of hatchery releases in the model is warranted at this time because hatchery release numbers have varied substantially in recent years, and it is possible that this variability will continue for the foreseeable future.

Table 1. Values of covariates used in the models. DD12 is the temperature covariate.

Brood year	Mgmt year	Return year	Empirical ETF	DD12	Natural-origin female spawners	Total female spawners	Hatchery pre-smolts
1996	1998	1999	0.213				
1997	1999	2000	0.398				
1998	2000	2001	0.267	6.63			153908
1999	2001	2002	0.218	0			30840
2000	2002	2003	0.261	13.79	3494	3501	166206
2001	2003	2004	0.206	41.13	5014	5289	252684
2002	2004	2005	0.274	5.63	5408	5711	233613
2003	2005	2006	0.230	12.51	4972	5217	218617
2004	2006	2007	0.209	80.21	3049	3293	168261
2005	2007	2008	0.185	50.49	7203	9049	173344
2006	2008	2009	0.154	0	7575	8860	196288
2007	2009	2010	0.211	51.27	1442	1551	71883
2008	2010	2011	0.175	163.31	1365	1461	146211
2009	2011	2012	0.335	107.4	2366	2723	198582
2010	2012	2013	0.375	2.94	692	824	123857
2011	2013	2014	0.486	0.86	426	491	194264
2012	2014	2015	0.269	0	880	1497	181857
2013	2015	2016	0.151	61.19	3400	3680	193155
2014	2016	2017	0.059	338.74	1399	1744	609311
2015	2017	2018	0.045	304.01	1592	2062	419690
2016	2018	2019	0.237	4.01	466	658	141332
2017	2019	2020	0.487	0	119	374	430292
2018	2020	2021	0.266	12.65	249	1087	406417
2019	2021	2022	0.177	0.09	3529	4950	417263
2020	2022	2023	0.117	37.68	2688	4018	516800
2021	2023	2024	0.025	316.19	5171	6200	651150

Table 2. Postseason escapement estimates and leave-future-out forecasts from each model.

Brood year	Mgmt year	Return year	E_3^0 yearly	E_3^0 mean	*Base* median/mode	*ETF* median/mode	*GP-1* median	*GP-2* median
1999	2001	2002	9042	8488				
2000	2002	2003	9732	9070				
2001	2003	2004	6329	5962				
2002	2004	2005	19518	18046				
2003	2005	2006	19569	18862				
2004	2006	2007	1857	2612				
2005	2007	2008	3022	2947				
2006	2008	2009	4483	4142				
2007	2009	2010	1344	1436				
2008	2010	2011	501	694				
2009	2011	2012	3523	3255	11530/5016	27897/11523	1606	1605
2010	2012	2013	6436	5946	3625/1540	12262/4259	3495	8478
2011	2013	2014	3163	3060	2623/998	26191/10471	5829	7013
2012	2014	2015	3990	3709	3754/1330	4319/2527	5488	3114
2013	2015	2016	843	865	5305/2061	1743/1261	2883	3437
2014	2016	2017	526	507	3244/1422	270/41	1254	2116
2015	2017	2018	2280	2112	2412/1250	156/70	715	715
2016	2018	2019	8757	8119	1594/660	1268/674	6476	6476
2017	2019	2020	7471	6918	1924/792	8619/3785	2935	2935
2018	2020	2021	11467	10883	3077/1266	4130/2174	7933	10963
2019	2021	2022	3997	6369	9063/3319	7069/3421	4313	4732
2020	2022	2023			5971/2338	2696/1405	4060	5262
2021	2023	2024			4540/1683	407/199	1062	1118

Table 3. Selection of predictors for *GP* model based on fit statistics for leave-future-out cross validation. The best values and selected best models are highlighted in bold. log sc = log scale

	Predictors	ME	RMSE	MPE	MAPE	MLAR	R^2	*r*	R^2 (log sc)	RMSE (log sc)
	logDD12, ETF, logSpawners, logHReleases	417.91	2452.86	21.53	70.47	-0.23	0.36	0.67	0.30	0.76
	ETF, logSpawners, logHReleases	1212.29	4102.69	26.62	97.81	-0.67	-0.78	0.06	-0.12	0.96
GP-2	**logDD12, logSpawners, logHReleases**	**14.44**	**2286.71**	50.08	93.05	-0.17	**0.45**	0.72	0.19	0.82
	logDD12, ETF, logHReleases	-577.82	2804.05	36.88	74.64	**0.00**	0.17	**0.73**	0.28	0.77
	logDD12, ETF, logSpawners	899.10	2938.06	27.80	82.01	-0.32	0.09	0.47	0.09	0.87
	logDD12, logHReleases	-372.31	2353.71	62.30	98.93	-0.06	0.41	0.71	0.20	0.81
	logSpawners, logHReleases	606.92	4463.14	163.04	222.53	-0.16	-1.11	-0.41	-0.93	1.26
	ETF, logHReleases	-198.43	4668.50	102.66	159.54	-0.48	-1.31	0.01	-0.36	1.06
	ETF, logSpawners	1212.33	4102.60	26.62	97.81	-0.67	-0.78	0.06	-0.12	0.96
GP-1	**logDD12, logSpawners**	801.49	2289.16	**20.35**	74.03	-0.32	**0.45**	0.72	**0.36**	**0.73**
	logDD12, ETF	-926.07	3674.38	31.31	**70.33**	0.33	-0.43	0.67	0.32	0.75
	logHReleases	712.94	4118.21	138.84	194.33	0.18	-0.80	-0.58	-0.69	1.18
	logDD12	-712.47	3105.72	46.25	83.24	0.14	-0.02	0.63	0.32	0.75
	logSpawners	1060.20	3971.90	73.64	133.13	-0.16	-0.67	-0.14	-0.42	1.08
	ETF	-52.37	3896.03	75.56	128.73	-0.45	-0.61	0.16	-0.10	0.95

Table 4. Fit statistics for each model for leave-future-out forecasts (return years 2012-2022).

Model	ME	RMSE	MPE	MAPE	MLAR	R^2	*r*
Base median	326.55	4642.27	98.86	149.33	0.01	-1.28	-0.16
Base mode	2917.18	4576.52	-17.30	85.09	-1.03	-1.22	-0.19
ETF median	-3834.64	10800.30	135.17	187.14	0.15	-11.35	-0.06
ETF mode	1048.82	5061.90	2.71	95.83	-0.60	-1.71	-0.05
GP-1	801.49	2289.16	20.35	74.03	-0.32	0.45	0.72
GP-2	14.44	2286.71	50.08	93.05	-0.17	0.45	0.72

Table 5. Fit statistics for each model for leave-future-out forecasts (return years 2015-2022).

Model	ME	RMSE	MPE	MAPE	MLAR	R^2	*r*
Base median	1138.63	4513.92	110.82	166.89	0.07	-0.68	-0.11
Base mode	3422.75	5045.10	-12.86	92.55	-0.84	-1.10	-0.18
ETF median	1488.50	3552.25	-16.53	54.92	-0.26	-0.04	0.51
ETF mode	3191.13	4411.94	-54.75	66.19	-1.12	-0.60	0.50
GP-1	935.64	2270.60	28.15	78.99	-0.27	0.58	0.82
GP-2	624.29	2023.62	53.72	100.14	-0.20	0.66	0.83

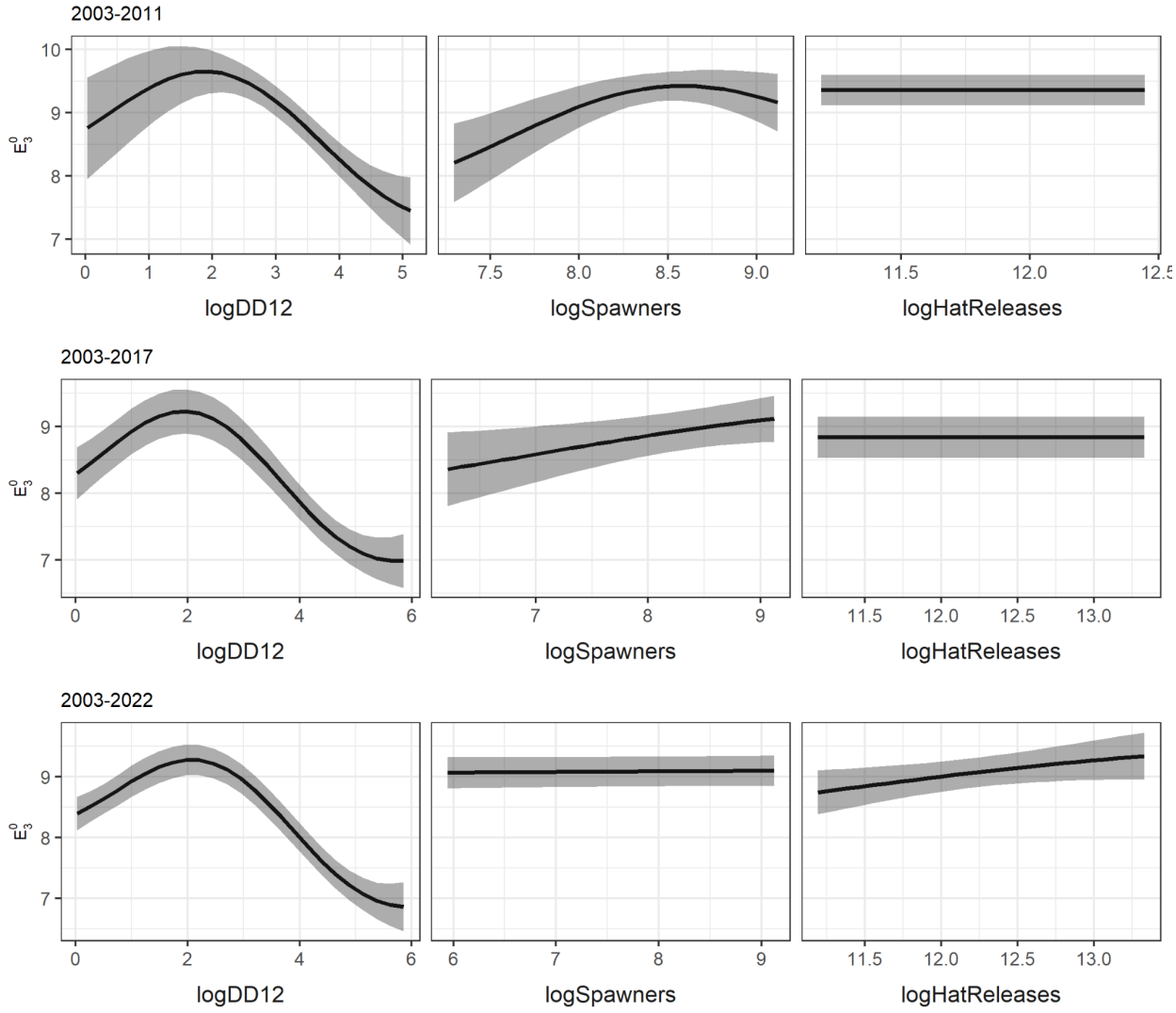

Figure 1. Conditional effects of each predictor in the *GP-2* model using differing amounts of training data (through return year 2011, 2017, and 2022), with other predictors fixed to their mean value (interactions among predictors are present but not shown). logDD12 is the temperature covariate. Conditional effects for the *GP-1* model, which does not include hatchery releases, resemble the first 2 columns.

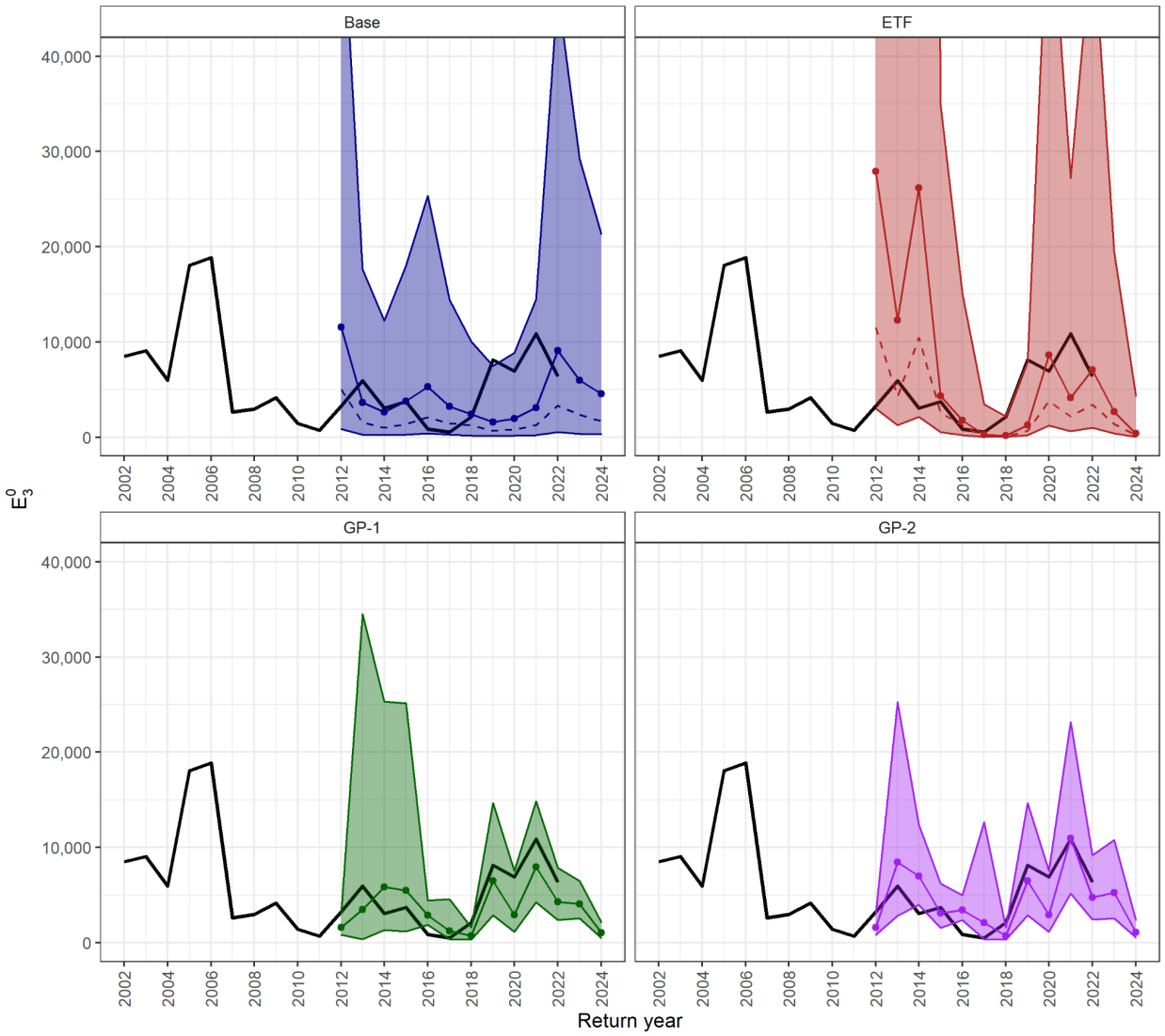

Figure 2. Postseason escapement estimates (black line) and leave-future-out forecasts (colored lines) from each model. Bands are 95% credible intervals (cropped in the *Base* and *ETF* models). Solid lines are medians and dashed lines (where plotted) are modes.

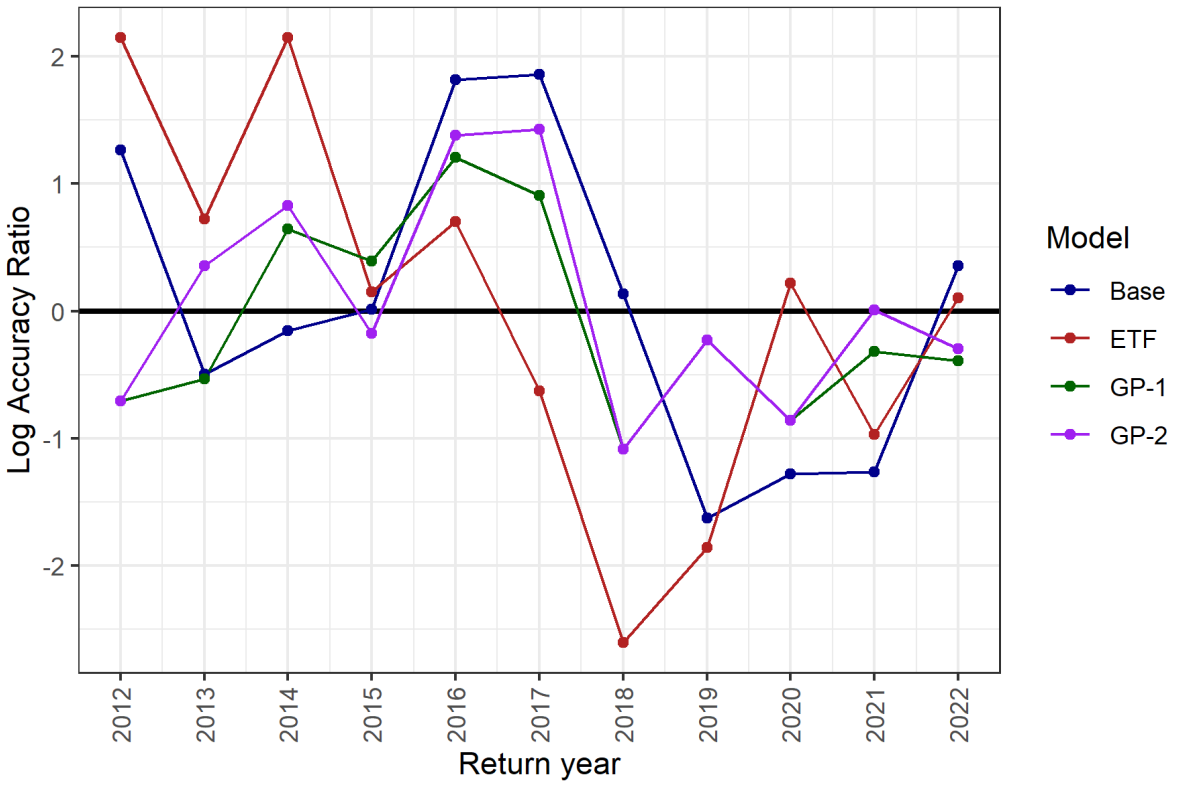

Figure 3. Log accuracy ratio, log(predicted/observed), for leave-future-out forecasts (medians) for each model.

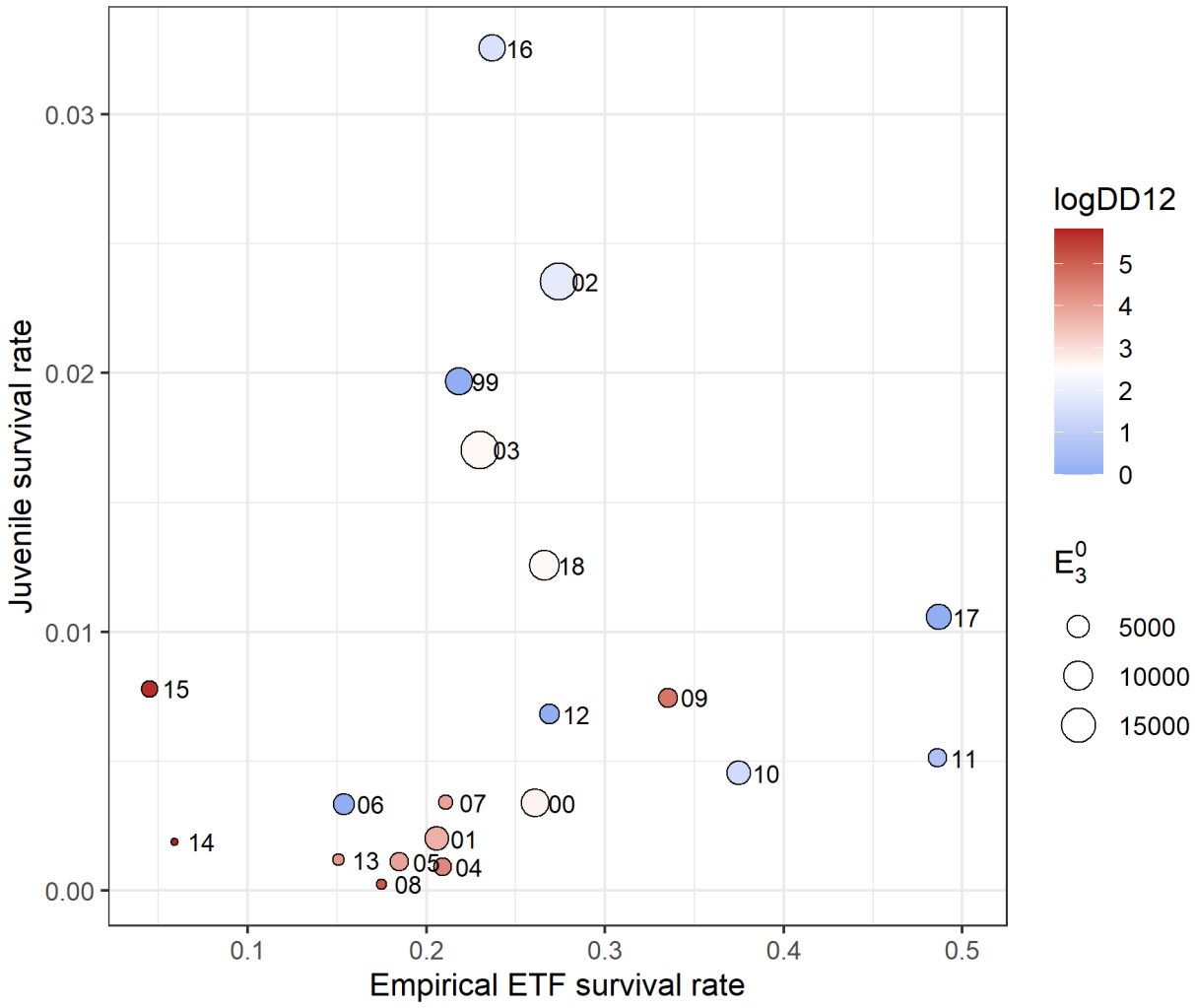

Figure 4. Hatchery-origin juvenile survival rate (fry to age-2) from the SRWC cohort reconstruction model vs. empirical ETF survival rate. Numbers next to points are brood years. logDD12 is the temperature covariate.

References

Blum, M. and Riedmiller, M. (2013) Optimization of Gaussian process hyperparameters using Rprop. Eur Symp Artif Neural Networks, Comput Intell Mach Learn Belgium:24–26.

Morley, S.K., Brito, T.V., and Welling, D.T. (2018) Measures of model performance based on the log accuracy ratio. Sp. Weather 16, 69–88. https://doi.org/10.1002/2017SW001669.

Munch, S. B., Poynor, V., and Arriaza, J. L. (2017) Circumventing structural uncertainty: a Bayesian perspective on nonlinear forecasting for ecology. Ecological Complexity, 32:134.

Munch S.B and Rogers T.L. (2022) GPEDM: Gaussian Process regression for Empirical Dynamic Modeling. R package version 0.0.0.9007. https://tanyalrogers.github.io/GPEDM

Neal, R.M. (1996) Bayesian Learning for Neural Networks (Springer-Verlag, NewYork)

O'Farrell, M. R., Mohr, M. S., Grover, A. M., and Satterthwaite, W. H. (2012). Sacramento River winter Chinook cohort reconstruction: analysis of ocean fishery impacts. U.S. Dept. Commer., NOAA Tech. Memo. NOAA-TM-NMFS-SWFSC-491, 68p.

O'Farrell, M.R. and Satterthwaite, W.H. (2015) Inferred historical fishing mortality rates for an endangered population of Chinook salmon (*Oncorhynchus tshawytscha*). Fishery Bulletin 113:341–351. doi: 10.7755/FB.113.3.9

O'Farrell, M., Hendrix, N., and Mohr, M. (2016) An evaluation of preseason abundance forecasts for Sacramento River winter Chinook salmon. Report prepared for the 2016 PFMC Salmon Methodology Review. https://www.pcouncil.org/documents/2016/11/agenda-item-d-2-attachment-1-an-evaluation-of-preseason-abundance-forecasts.pdf/

PFMC (2018) Preseason Report I: Stock Abundance Analysis and Environmental Assessment Part 1 for 2017 Ocean Salmon Fishery Regulations. (Document prepared for the Council and its advisory entities.) Pacific Fishery Management Council, 7700 NE Ambassador Place, Suite 101, Portland, Oregon 97220-1384.

Poytress, W. R. (2016) Brood-year 2014 winter Chinook Juvenile Production Indices with comparisons to Juvenile Production Estimates derived from adult escapement. U.S. Fish and Wildlife Service, Red Bluff Fish and Wildlife Office, 10950 Tyler Road, Red Bluff, CA, 96080.

Rasmussen, E. and Williams, K. I. (2006) Gaussian Processes for Machine Learning. MIT Press.

Satterthwaite, W.H. and Shelton, A.O. (2023) Methods for assessing and responding to bias and uncertainty in US West Coast salmon abundance forecasts. Fisheries Research, 257, p.106502.

Voss, S. D. and Poytress, W. R. (2022) 2020 Red Bluff Diversion Dam Rotary Trap Juvenile Anadromous Fish Abundance Estimates. Report of U.S. Fish and Wildlife Service to U.S. Bureau of Reclamation, Sacramento, CA.

Winship, A.J., O'Farrell, M.R., and Mohr, M.S. (2014) Fishery and hatchery effects on an endangered salmon population with low productivity. Transactions of the American Fisheries Society 143:957-971. doi: 10.1080/00028487.2014.892532

An evaluation of preseason ocean abundance forecasts for

Oregon Production Area hatchery Coho salmon

Cassie Leeman; Oregon Department of Fish and Wildlife, cassandra.r.leeman@odfw.oregon.gov

Shannon Conley, Mark Sorel, Thomas Buehrens; Washington Department of Fish and Wildlife

September 27, 2023

Executive Summary

Fishery planning and adaptive management for Coho salmon (*Oncorhynchus kisutch*) stocks along the Pacific Coast depend upon reliable preseason forecasting. The largest Coho salmon management area governed by the Pacific Fishery Management Council (Council) is the Oregon Production Index (OPI) area. OPI natural and hatchery origin Coho originate from stocks produced in rivers between Leadbetter Point, Washington and the US/Mexico border. For management purposes this area is broken into three stocks: the Oregon Coast Natural (OCN), Lower Columbia Natural (LCN), and Oregon Production Index Hatchery (OPI-H) stocks. The current forecasting methodology for OPI-H was reviewed in 2021 by the Council (Suring and O'Farrell, 2021). However, analyses exploring forecast approaches of OPI-H abundance were last conducted in 1996. Due to the history of the model analysis and a decrease in model performance in recent years, the Council has asked the OPI Technical Team (OPITT) to explore alternative approaches for the OPI-H Coho forecasting.

In support of the Council's request for review, this document explores alternative forecasts for pre-fishing adult ocean abundance of OPI-H Coho and compares the performance of these models to the current forecast methodology. Our alternative approach differs from the current approach in multiple ways; it assumes a log-linear relationship between OPI-H abundance and covariates, incorporates covariates that reflect conditions in the marine environment, uses autoregressive integrated moving average (ARIMA) error structures, and employs multi-model (ensemble) predictive inference. We found that the alternative approach would have produced considerably smaller forecasting errors on average over the past 15 years than the current forecasting approach. We conclude by recommending that the Council adopt the alternative approach due to the results of our simulation of historical performance and the greater flexibility of the alternative approach to adapt to the demonstrated non-stationary relationship between OPI-H Coho abundance and explanatory variables.

Background

In 2021, the current OPI-H forecast methodology was presented to the Council salmon subcommittees for review (Suring and O'Farrell, 2021). A linear model predicts the adult pre-fishing ocean abundance in year t from jack returns to OPI area basins in year t-1 and variable relating delayed smolt releases to jack abundance in year t-1. Conclusions from the 2021

methodology review report demonstrate that the current forecast methodology ranked third best among the nine Council managed Coho stocks for mean absolute percent error (MAPE) and best for relative mean absolute error (RMAE). These results indicate the performance of the current forecasting method ranks favorably compared to other methodologies used in Council managed Coho stocks. The analysis reported that the forecast model fit the entire dataset well and the prediction error was unbiased. However, the report noted the model fit older data better than more recent data and that the adjusted R^2 value declined over time. Patterns in the t-value results for individual regression components indicated that the delayed smolt adjustment metric has been a less predictive indicator in more recent timeframes than in the past. The report also stated concerns that the current method may be less informative in recent years due to changes in the marine environment and hatchery practices.

Adult salmon abundance is often related to the survival of earlier maturing individuals in the same cohort (e.g., jacks) and environmental conditions present during various life history stages. The current model exclusively considers jack returns and smolt releases, yet environmental conditions have an impact on salmon life history and may be valuable predictors in salmon abundance forecasting. Environmental conditions such as the timing and strength of upwelling in the California Current, north pacific gyre oscillation (NPGO), El Niño southern oscillation (ENSO), sea surface temperature (SST), and sea surface height (SSH) are associated with Coho salmon abundance (Rupp et al., 2012). Notably, higher SST and weaker upwelling events were projected to negatively impact the survival rates of salmon populations (Crozier et al., 2021). For OCN Coho, the timing of the spring transition to upwelling in the California Current, Multivariate ENSO Index, upwelling winds, SSH, and SST were significant abundance predictors (Rupp et al., 2012). An increased average global SST, more frequent marine heatwaves, and higher variance in circulation events generated through climate change may reduce the predictive power of traditional indicators of abundance; as such we assess how incorporating environmental data impact the forecasting of OPI-H Coho abundance (NOAA, 2021; Litzow et al., 2020; Cheung and Frölicher, 2020).

There has not been a Council-reviewed analysis that explores alternative forecasting approaches or addresses the concerns noted in the 2021 OPI-H methodology review report to date. The Council's request to explore alternative forecasting approaches of OPI-H provides an opportunity for the OPITT to expand on the analysis reported to the Council in 2021. The objective of this review is to evaluate the bias and precision of alternative forecast approaches for the pre-fishing adult ocean abundance of OPI-H Coho and compare them to the current forecasting methodology to improve preseason forecasting.

Methods

Stock description

The Oregon Production Index hatchery (OPI-H) Coho abundance forecast, a misnomer, includes all hatchery production in the OPI area (Leadbetter Point, WA to US/Mexico border) and all naturally produced Coho from the Columbia River basin. After the total OPI-H forecast is produced, it then gets broken down into individual model stock components for input into the preseason Coho Fishery Regulation Assessment Model (FRAM). The scope of this methodology review is limited to exploring alternative forecast approaches of the total OPI-H abundance and does not include alternative forecast approaches of the individual model stock components of OPI-H Coho.

Postseason abundance estimates of the OPI-H components are generated by cohort reconstruction, including all fishery impacts, using a Mixed Stock Model (MSM; Packer et al., 2007). In 2008, OPI-H postseason abundance estimates shifted from a stratified random sampling (SRS) approach to the MSM. This change to the methodology improved overall accounting of total harvest and mortality of OPI-H Coho and became consistent with the methods used in the base period of Coho FRAM (PFMC, 2023). In 2011, analysis suggested the abundance estimates from the MSM were equivalent to the SRS time series and MSM data was determined as best available data starting in 1986 (Suring and O'Farrell, 2021). Annual MSM OPI-H Coho abundance estimates are published in Table C-2 of the Council's Preseason Report I.

Current forecast methodology

The current forecast approach was implemented in 1996 with a modification to the jack returns covariate in 2008 (PFMC, 2023). A multivariate linear regression model assuming normal errors is fit to the most current data t is forecasted using jack and smolt production estimates from year $t-1$ (See Table A4 for the jack and smolt datasets and Table A2 and A3 for a list of facilities these values are derived from). The model is:

$$Eq.\ 1. \quad y_t = a(JackOPI_t) + b\left(JackCR_t \cdot \left(\frac{SmD_{t-1}}{SmCR_{t-1}}\right)\right) + \varepsilon_t$$

where y_t is OPI-H abundance in year t, Jack OPI is the jack returns to all OPI hatcheries, Jack CR is the jack returns to Columbia River hatcheries, SmD is the delayed smolts release from Columbia

River hatcheries, and SmCR is the total smolts released from Columbia River hatcheries. The third term in this equation, referred to as the "delayed smolt adjustment index", is intended to address the effect of variable proportions of delayed release smolts on the jack to adult ratio (Suring and O'Farrell, 2021). Finally, ε_t is a normally distributed residual with a mean of zero. Code and the data used for this forecasting can be found at https://github.com/ErikSuring/OPIH_Evaluation. Further documentation of the current OPI-H forecast methodology approach can be found in the OPI-H methodology review summary report submitted to the Council in 2021 for review (Suring and O'Farrell, 2021). Documentation for annual forecasts can be found in the Council's Preseason Report I (PFMC, 2023).

Forecasting Methods Evaluated

Overview

We evaluated a methodology of constructing ensemble forecasts (Dormann et al., 2018), where individual models in the ensemble have ARIMA components and covariates. We fit many different models with different combinations of covariates, then evaluate the performance of individual models, and finally develop ensembles of top-performing models. The approach is designed to identify models or ensembles with the highest out-of-sample one-step-ahead forecasting performance, and in doing so eliminate the tendency to overfit the in-sample data by considering many models. The steps in this procedure were as follows:

1) Identify a set of covariates and a minimum and maximum number of covariates to include in each individual model,
2) Fit ARIMA models with all unique combinations of covariates to subsets of the data and make one-step-ahead forecasts,
3) Calculate one-step-ahead performance metrics for unique combinations of covariates across forecast years,
4) Generate performance-weighted ensemble forecasts by taking the weighted-mean of a top-performing subset of models
5) Evaluate how well forecasts would have performed:
    a. if each of the ensemble approaches had been used in the past 15 years

b. if the best performing individual model (based on the prior 15 years of one-step-ahead performance) had been used.

c. if the current model had been used in the past 15 years

Step 1. Identifying the covariate set

We included 11 covariates in our forecasting, included jack returns and the delayed smolt adjustment metric used in the current approach, as well as nine environmental variables (Table 1). Six of the environmental covariates explored are covariates used within the OCN forecast methodology; May-July PDO, October-December Multivariate Enso Index, July-September Upwelling Index, April-June SST, April-June Sea Surface Height, and September-November Upwelling Index (Table 1). Further information of the covariates used in OCN forecasts can be found in Rupp et al., 2012. For new ARIMA models and ensembles, OPI jack abundance was log-transformed because these models were fit using a log-link (as opposed to the current methodology using an identity-link). The adjusted smolt metric was also modified by log-transforming CR jack abundance in its calculation:

Eq. 2. $lag1\_log\_SmAdj = \log(lag1.JackCR) * (lag1.SmD/lag1.SmCR)$

In order to compare performance of the new methods with the current methods, the current methods were fit with these variables un-modified as shown in Equation 1.

Table 1. Covariates explored for model analysis.

Predictor variable	**Abbreviation**	**Data Source**
OPI-H jack abundance; year t-1; log-transformed	lag1_log_JackOPI	Erik Suring (ODFW): https://raw.githubusercontent.com/ErikSuring/OPIH_Evaluation/main/PUB2023.txt
OPI-H adjusted smolt metric; year t-1; lagged t-1 and log transformed	lag1_log_SmAdj	Erik Suring (ODFW): https://raw.githubusercontent.com/ErikSuring/OPIH_Evaluation/main/PUB2023.txt
North pacific gyre oscillation; year t-1	Lag1_NPGO	http://www.o3d.org/npgo/npgo.php

Table 1. Continued.

Pacific decadal oscillation; year t-1	**Lag1_PDO**	**https://psl.noaa.gov/pdo/data/pdo.timeseries.ersstv5.csv**
Winter sea surface temperature; Average October-January	WSST_A	https://www.ncdc.noaa.gov/data-access/marineocean-data/extended-reconstructed-sea-surface-temperature-ersst-v5 average over box from 44˚N–50˚N latitude and 120˚W–125˚W longitude
Pacific decadal oscillation; May, Jun., Jul.	PDO.MJJ	https://psl.noaa.gov/pdo/data/pdo.timeseries.ersstv5.csv
Multivariate ENSO Index; Oct., Nov., Dec.	MEI.OND	https://psl.noaa.gov/gcos_wgsp/Timeseries/Data/nino34.long.anom.data
Upwelling Winds Index; Jul., Aug., Sep.	UWI.JAS	Erik Suring (ODFW) from R script used in OCN forecast; http://orpheus.pfeg.noaa.gov/outgoing/upwell/monthly/upindex.mon.
Sea surface temperature; Apr., May, Jun.	SST.AMJ	Erik Suring (ODFW) from R script used in OCN forecast; http://opendap.co-ops.nos.noaa.gov/dods/IOOS/Water_Temperature.html.
Sea surface height; Apr., May, Jun.	SSH.AMJ	Erik Suring (ODFW) from R script used in OCN forecast; http://ilikai.soest.hawaii.edu/uhslc/datai.html.
Upwelling Winds Index; Sep., Oct., Nov.	UWI.SON	Erik Suring (ODFW) from R script used in OCN forecast; http://orpheus.pfeg.noaa.gov/outgoing/upwell/monthly/upindex.mon.

Step 2: Fitting models and forecasting

For this analysis, we explored forecasting with 1,485 unique covariate combinations,

Eq. 3. $\sum_{k=min}^{max}\binom{C}{k} = 1{,}485$

where k is the number of unique covariates in a combination, $C = 11$ is the total number of covariates considered, and *min* and *max* were set to 0 and six, respectively, governing the number of covariates allowed in combinations. This resulted in 1,485 unique combinations of covariates. We fit ARIMA models with each combination of covariates to subsets of the data beginning with the first year of post-season run size estimates ($t_0 = 1970$) and running through subsequent year $t \in \{2007, 2008, 2009 \ldots 2022\}$. We used each ARIMA model to forecast the run size in year $t + 1$ such that we generated 1,485 unique one-year-ahead forecasts for years 2008–2023. This allowed us to evaluate the performance of models with different combinations of covariates in forecasting returns in the 15 most recent years (2008-2022) and generate a forecast for the upcoming year (2023) for which the post-season run size is unknown.

The structure of the auto-regressive, differencing, and moving-average components of each model (covariate combination and data subset) were selected based on $AICc$ using the function *auto.arima* within the forecast R package (Hyndman et al., 2023; Hyndman et al., 2008). The generic ARIMA model we used with no differencing and lag-1 autoregressive and moving average components can be written as:

Eq. 4. $\log(y_t) = \mu_t + \phi_1(\log(y_{t-1}) - \mu_{t-1}) + \theta_1\varepsilon_{t-1} + d + \varepsilon_t$

where y is the observed abundance in year t ($OPIH_t$), which after log transformation is equal to the sum of the log-mean abundance μ_t in year t, an autoregressive error term where $\phi_1$is multiplied by the difference between the log of the observed abundance and log-mean abundance in year $t - 1$, a moving average error term where θ_1 is multiplied by the residual from the previous year, a drift term d, which is a linear trend (on the log scale), and a residual ε_t which is normally distributed around zero. The log-mean in year t is estimated by multiple linear regression:

Eq. 5. $\mu_t = \boldsymbol{Xb}$

where $\boldsymbol{X}$ is a design matrix of covariates with rows equal to the number of years, and columns equal to the number of covariates in a particular model, while $\boldsymbol{b}$ is a vector of coefficients corresponding

to the covariates. The first column of $\boldsymbol{X}$ is equal to 1 corresponding to the first coefficient in vector $\boldsymbol{b}$, which is the intercept. Bolding indicates matrix multiplication.

The function *auto.arima* implements an algorithm that fits variations of Equation 4 to the data, all of which include the residual error and mean terms, but which either includes or does not include the autoregressive, moving average, and drift components. It also fits versions of the equation where the observations are subject to differencing using the backshift operator and evaluates whether additional autoregressive and moving average terms for different lags (other than lag 1 shown above) improve model fit. To assess model fit, *auto.arima* compares the $AICc$ value of each of the models it fits, selecting the model with the best combination of autoregressive, moving average, drift, and differencing for the particular set of data it is fit to. For purposes of simplicity, the differencing and multi-model evaluation within *auto.arima* is not shown in Equation 4 but full details of the *auto.arima* function are available in Hyndman et al., 2023 and Hyndman et al., 2008.

Step 3: Performance evaluation for unique covariate combinations (i.e., individual models)

We assessed the forecast performance of models with each combination of covariates, i, based on their mean absolute prediction error (MAPE; Equation 6), root mean square error (RMSE; Equation 7), and mean symmetric accuracy (MSA; Equation 8), over the most recent 15 years for which abundance data were available:

$$Eq.\ 6.\ MAPE_i = \frac{\sum_{t=2008}^{2022}(\hat{y}_{i,t}-y_t)/y_t}{15} * 100,$$

$$Eq.\ 7.\ RMSE_i = \sqrt{\frac{\sum_{t=2008}^{2022}(\hat{y}_{i,t}-y_t)^2}{15}},$$

$$Eq.\ 8.\ MSA_i = \left[\exp\left(\frac{\sum_{t=2008}^{2022}|\log(y_t/\hat{y}_{i,t})|}{15}\right)-1\right]*100,$$

where y_t is the postseason estimate of abundance in year t and $\hat{y}_{i,t}$ is a preseason forecast. For all performance error metrics, a lower value is indicative of a higher forecasting accuracy.

Step 4: Generating ensemble forecasts

We generated ensemble forecasts by taking weighted means (harmonic means) of the $M = 10$ models with the lowest MAPE.

Eq. 9. $\hat{y}_t = \frac{\sum_i \omega_i \hat{y}_{i,t}}{M}$

We calculate weights in four different ways to generate four different ensemble forecasts. Three of the ways were calculated by normalizing the inverse of a performance metric, p_i , of each model:

Eq. 10. $w_i = \frac{(p_i)^{-1}}{\sum_{i=1}^{M}(p_i)^{-1}}$

where the performance metrics were MAPE, RMSE, and MSA. The final method of generating weights was to use a Markov-Chain Monte-Carlo optimization algorithm that minimized the MAPE of the ensemble forecasts across 2008–2022, termed stacking weights (Smyth and Wolpert 1999).

Step 5: Evaluating forecast performance

We evaluated the performance of the current OPI-H forecasting methodology, the four different approaches to generating ensemble forecasts, and an approach of choosing a single best individual covariate combination (as measured by MAPE in the previous 15 years) to use for forecasting returns in each individual year. We simulated the performance of the current OPI-H forecasting methodology by refitting the model to expanding windows of the dataset, just as we did to simulate the performance of individual ARIMA models. For the ensemble approaches and selecting the best individual ARIMA model with covariates, we repeated the 4-step processes described above to forecast returns in 2008–2022, where the models used to forecast returns in a given year had no access to the observed returns in that year. Thus, when generating ensemble weights or selecting the best individual model to forecast 2008 abundance we considered the performance of individual models in 1993–2007, when generating a forecast for 2009 we considered the performance of individual models in 1994–2008, and so on. Finally, calculated the performance metrics shown above for each approach over the 2008 to 2022 period.

Results

The best performing ensemble model, and best performing modeling methodology considered was the MAPE-weighted ensemble, which had a MAPE of 36.48, RMSE of 173.47, and MSA of 37.62 (Table 2). The current OPI-H methodology had the highest errors of the approaches evaluated, with a MAPE of 61.73, an RMSE of 352.20, and an MSA of 66.06. The four ensemble models and the approach of selecting the best individual ARIMA model annually had relatively similar performance across the years evaluated. Notably, the difference in MAPE between the best-performing ensemble approach (MAPE weighted) and the worst-performing of the new methodologies reviewed (choosing the best individual model) was 1.48, whereas the difference between the MAPE-weighted ensemble and the current OPI model was 25.25.

Table 2. Performance of modeling approaches based on 15 years of out-of-sample one-step-ahead cross validation. Approaches include selecting a single best individual ARIMA model each year (Best individual) as well as weighted ensembles and the current OPI-H forecasting model (Current OPI). Ensembles include a "stacking weight" ensemble where an optimization algorithm is used to identify the weights that maximize out-of-sample one-step-ahead performance over a sliding 15-year window (Stack weighted), as well as more traditional ensembles using a harmonic mean where model weights are calculated based on skill measured by RMSE (RMSE weighted), MAPE (MAPE weighted), or MSA (MSA weighted).

MAPE	RMSE	MSA	Model
36.48	173.47	37.62	MAPE weighted
36.55	173.39	37.82	MSA weighted
37.12	174.42	38.79	RMSE weighted
37.97	171.92	40.23	Stack weighted
38.06	187.63	45.47	Best individual
61.73	352.20	66.06	Current OPI

In addition to performing similarly in terms of precision, the ensemble models and choosing the best individual covariate combination annually produced similar forecasts (Figure 1), with the greatest variance across approaches in 2008. The current OPI-H approach was generally more different from the multi-model approaches than the multi-model approaches were from one another, and the current approach diverged from the other approaches considerably in 2021 and 2022. The MAPE weighted ensemble approach under-predicted abundance in 2021–2022 but was closer to the observed abundance than the current OPI-H approach in those years.

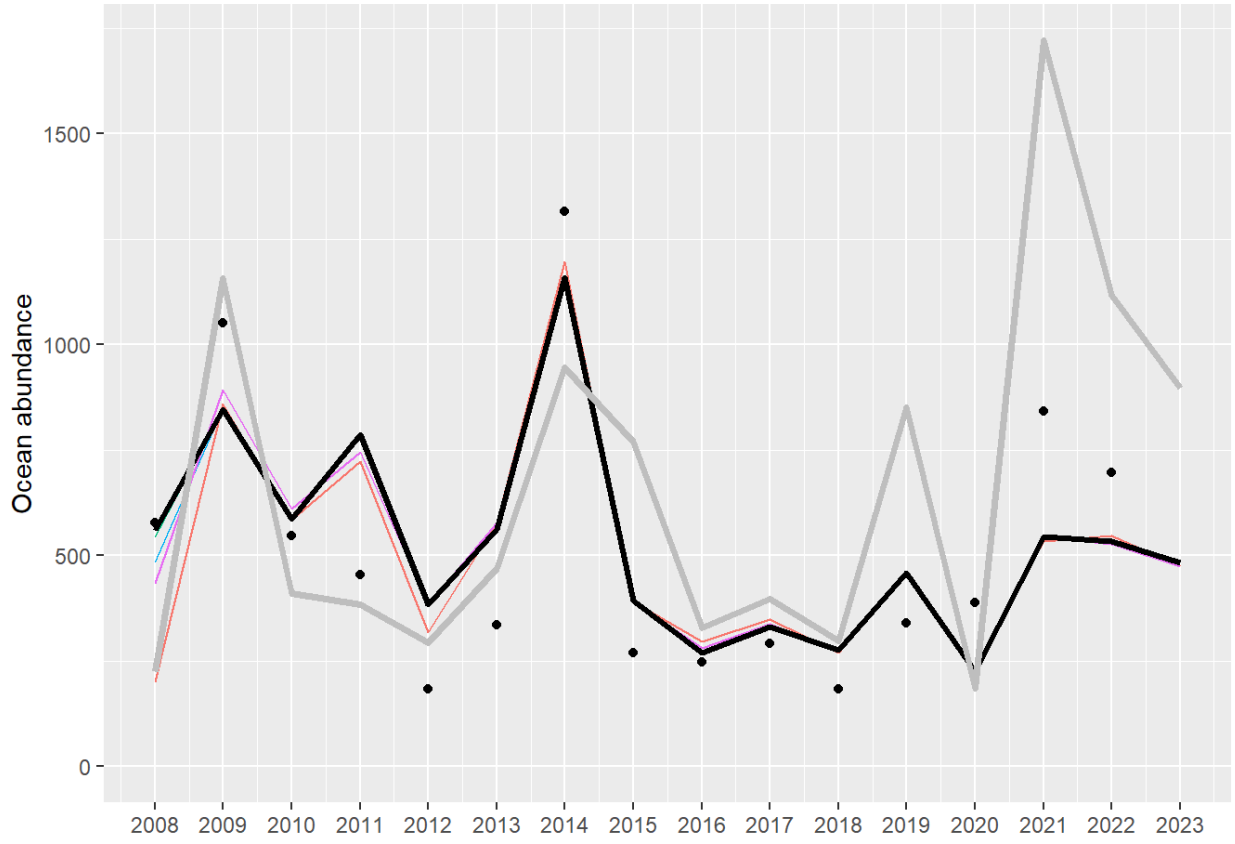

Figure 1. One-step-ahead predictions (lines) of total OPI Coho abundance for each year's top individual and weighted ensemble model set (colored lines), the MAPE weighted model (black line), and the current OPI-H model (gray line) relative to observed abundance (black dots).

The mean percent forecast error from 2008 to 2022 for the current forecast and MAPE weighted methodologies are 37.5% and 18.6%, respectively (Figure 2). Both the current and MAPE weighted methodology have over-predicted the abundance for 10 of the past 15 years (Figure 2). However, the MAPE weighted method has consistently less error than the current methodology, with the exception of the years 2011, 2012, and 2013. We do not believe the MAPE-weighted approach is a biased estimator; rather that 15 years is a small sample size to assess accuracy. Using a beta distribution to estimate the proportion of years the MAPE-weighted ensemble forecast is above or below the true abundance based on our sample size of 10 forecasts above and 5 below, we obtain a 95% CI of 0.38-0.88, indicating no significant difference (p = 0.30) from the expected value of 0.5 for an unbiased estimator.

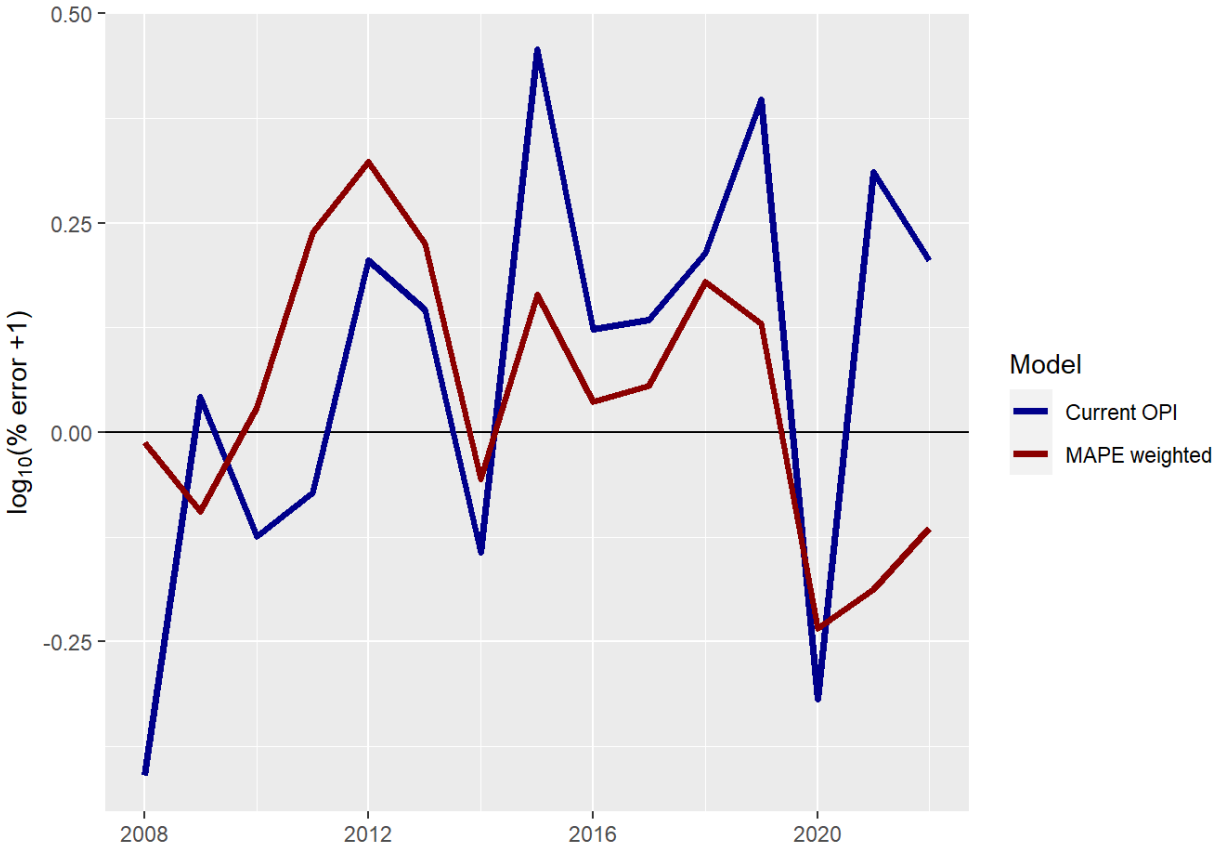

Figure 2. Log_{10} of percent forecast error plus 1 of the MAPE weighted and current forecast models through time. The transformation to the percent error was made so that the distribution of errors was less skewed because negative percent errors cannot be less than one whereas positive errors can be any magnitude.

In addition to assessing the accuracy [bias] and precision of forecast point estimates, we assessed the performance of prediction intervals. The post-season estimate of abundance was within the 95% prediction interval for the MAPE weighted ensemble for 14 of the 15 (93.33%) of years assessed and within the 50% prediction interval for 6 of the 15 (40%) of years assessed, indicating that the nominal coverage of the prediction intervals was similar to their true coverage. The true coverage was not statistically different from the nominal coverage in either case.

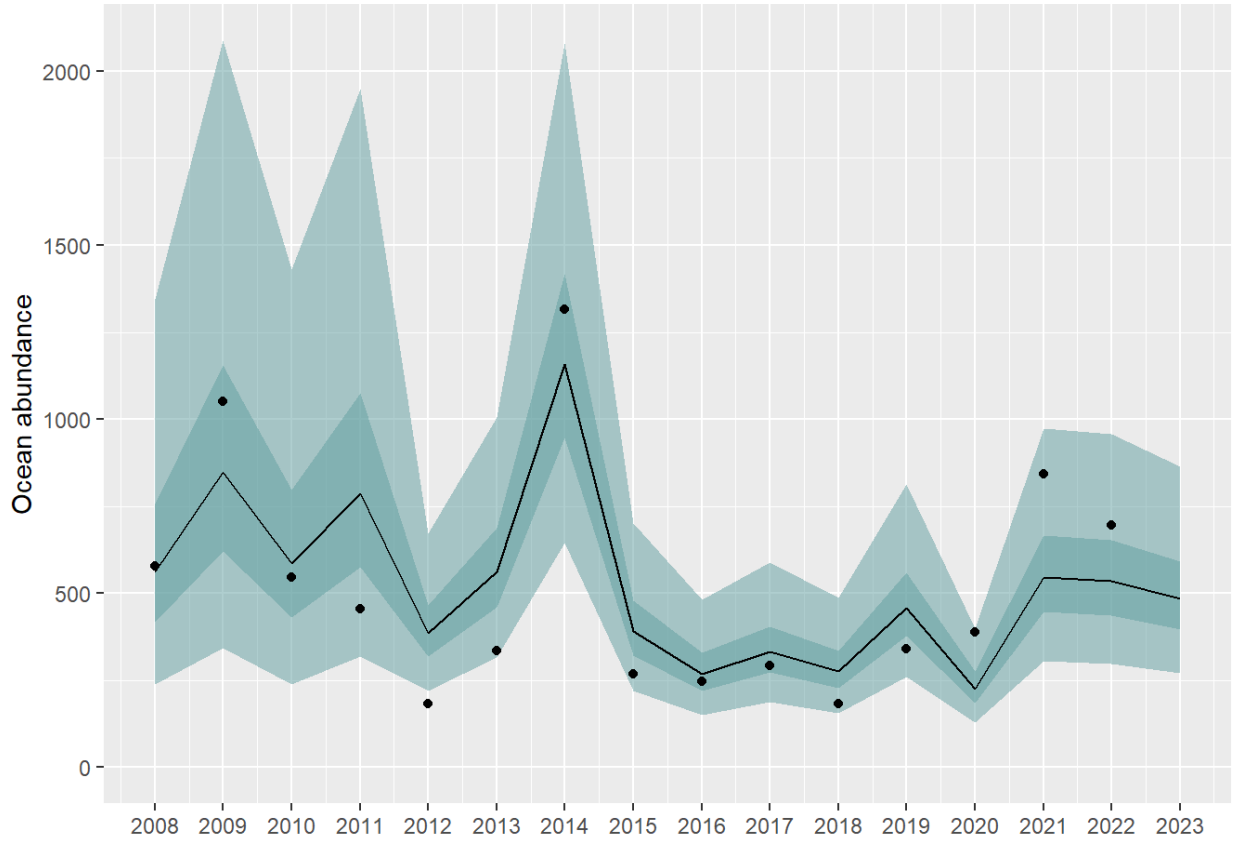

Figure 3. One-year-ahead predictions (black line) of total OPI Coho abundance from the MAPE weighted model relative to observed abundance (black dots). Prediction intervals are shown as blue shading including 50% (dark), 95% (light).

To provide a sense of what covariate combinations have performed best in forecasting returns in the recent past, Table 3 shows the individual model that would have been chosen each year based on a 15-year retrospective evaluation. The covariates within the best models explored

for each year highlights the dynamic nature of environmental covariates in forecasting OPI-H Coho. From 2008 to 2011, the variation in covariates is greater than in models from 2012-2023. There is only one year (2008) where the jack return (lagged and logged) and adjusted smolt metric (lagged and logged) are both included as covariates. Since 2012, jack returns (lagged and log transformed), NPGO (lagged), PDO (lagged), and WSST are consistently present in the models with MEI (Oct., Nov., Dec.) becoming more present in the top models starting in 2014.

Table 3. Best-performing covariate combinations based on one-year-ahead MAPE in a 15-year retrospective analysis and their forecasts.

Year	Model	Predicted abundance	Lo 50	Hi 50	Lo 95	Hi 95
2008	lag1_log_JackOPI + lag1_log_SmAdj + lag1_NPGO + WSST_A + PDO.MJJ + SSH.AMJ	201.27	171.95	235.58	127.39	317.99
2009	lag1_log_SmAdj + lag1_NPGO + UWI.JAS + SSH.AMJ + UWI.SON	859.74	628.29	1176.46	345.59	2138.81
2010	lag1_log_SmAdj + lag1_NPGO + UWI.JAS + SSH.AMJ + UWI.SON	585.46	429.62	797.83	238.18	1439.10
2011	lag1_log_SmAdj + lag1_NPGO + lag1_PDO + MEI.OND + UWI.JAS + SSH.AMJ	724.33	533.81	982.84	298.38	1758.34
2012	lag1_log_JackOPI + lag1_NPGO + lag1_PDO + WSST_A + PDO.MJJ + UWI.SON	319.03	262.56	387.64	181.13	561.91
2013	lag1_log_JackOPI + lag1_NPGO + lag1_PDO + WSST_A + PDO.MJJ	578.32	476.01	702.61	328.46	1018.23
2014	lag1_log_JackOPI + lag1_NPGO + lag1_PDO + WSST_A + PDO.MJJ + MEI.OND	1196.39	977.87	1463.75	665.80	2149.82
2015	lag1_log_JackOPI + lag1_NPGO + lag1_PDO + WSST_A + PDO.MJJ + MEI.OND	390.64	319.65	477.39	218.11	699.64
2016	lag1_log_JackOPI + lag1_NPGO + lag1_PDO + WSST_A + MEI.OND + UWI.SON	295.22	240.13	362.94	161.99	538.01
2017	lag1_log_JackOPI + lag1_NPGO + lag1_PDO + WSST_A + MEI.OND + UWI.SON	348.40	283.96	427.46	192.30	631.22
2018	lag1_log_JackOPI + lag1_NPGO + lag1_PDO + WSST_A + MEI.OND	270.52	222.81	328.44	153.94	475.39
2019	lag1_log_JackOPI + lag1_NPGO + lag1_PDO + WSST_A	457.36	376.78	555.18	260.42	803.24
2020	lag1_log_JackOPI + lag1_NPGO + lag1_PDO + WSST_A + MEI.OND	228.87	188.37	278.08	129.96	403.06
2021	lag1_log_JackOPI + lag1_NPGO + lag1_PDO + WSST_A + MEI.OND	533.36	437.28	650.55	299.47	949.90
2022	lag1_log_JackOPI + lag1_NPGO + lag1_PDO + WSST_A + MEI.OND	547.05	447.79	668.31	305.75	978.80
2023	lag1_log_JackOPI + lag1_NPGO + lag1_PDO + WSST_A + MEI.OND	475.39	389.56	580.13	266.54	847.89

Discussion

This review represents the first exploration of alternative forecast approaches to OPI-H Coho in over two decades. This renewed interest was triggered by current forecast methodologies becoming less precise through time, which is hypothesized to be due to the lack of ability to capture the variability of environmental conditions and changes in the proportion of the population

returning as jacks through time (Suring and O'Farrell, 2021). We demonstrated that a multi-model approach utilizing ARIMA model structures and environmental predictors would have performed better than the current OPI-H Coho forecasting approach over the last fifteen years. The new methodology incorporates information on ocean conditions that affect survival, models abundance in log space, includes ARIMA error structures, and should be more adaptive from year to year than the current method.

Our results suggest that incorporating information on marine conditions that affect survival can contribute additional predictive power, beyond what is provided by just including jack returns. Our findings indicate that NPGO and PDO, which were included in all of the top-performing models, contribute information about marine survival that is not captured by jack returns. This may be due in part to interannual variability in the proportion of fish returning as jacks or measurement error in jack returns. The winter sea surface temperature covariate reflects conditions that would impact survival during fish's second winter at sea, after jacks have already returned, and thus provides more recent information that is not reflected in jack returns. Winter sea surface temperature was included in 13 out of 16 of the annually top-performing models, demonstrating how including environmental indices in forecast models, and particularly those that capture near-term changes, can provide valuable information beyond that included in sibling returns from previous years to improve prediction. Even the worst performing of the new models that we evaluated was substantially better-performing than the current OPI-H forecasting model, demonstrating the advantages of including environmental covariates in forecasting models.

The proposed forecasting approach differs from the current approach in that it assumes a log-linear relationship between adult abundance and jack returns and uses ARIMA error structures. Abundance can only be positive, so it should be modeled in log space to constrain predictions to the positive domain. Additionally, the use of a log-link assumes heteroskedastic errors (i.e., larger variance with larger abundance) which has been observed in the OPI-H and other salmon abundance datasets. The log-link also assumes relationships between covariates and abundance are multiplicative rather than additive, which better matches generative processes for abundance (e.g., survival, which is multiplicative). In addition to fitting adult abundance on a log-link scale, we log transformed the jack covariate such that we modeled a linear relationship between adult abundance and jack returns when jack returns were included as a covariate in a model. Finally, because the ARIMA structure allows for time-varying error in the log-linear predictor, it functionally allows for modeling a time varying relationship between covariates like jack returns and expected adult abundance (i.e., when exponentiated, the intercept is multiplied by the

autoregressive and moving average error terms, and by the jack covariate, in effect allowing for a time-varying jack to adult ratio).

Importantly, the multi-model forecasting approach and use of an ARIMA structure that can change across years allows for the alternative forecasting model to adapt to changing age structure and relationships between ocean indices and adult abundance. A challenge with choosing a single covariate combination to use for forecasting is that the information contained in those covariates may become less predictive through time and other covariate combinations may become more predictive. This is illustrated in our finding that the covariates included in the best individual model changed over the 2008 to 2022 period. Given the time constraints of agency staff and Council members, forecast methodologies can go many years without being reviewed. Therefore, it is advantageous to adopt methodologies that are highly flexible and can adapt to changing relationships through time. Our approach accomplishes this by systematically evaluating the performance of many combinations of covariates in the recent past, generating ensembles of the best-performing models to use for forecasting adult abundances in a subsequent year. While the multi-model ensemble approach allows the covariates and ARIMA structure to change across years, the systematic way in which the covariate combinations and ARIMA structure are determined allowed us to simulate how it would have performed in the recent past. The results of this simulation suggest that the multi-model ensemble approach performed substantially better than the current OPI-H modeling approach on average over the last 15 years, although there were three years in which the current OPI-H model performed better than the multi-model approach.

In considering whether to adopt a multi-model ensemble approach to forecasting OPI-H Coho, it may be useful to consider that such an approach has been used in the past by the U.S. v. OR Technical Advisory Committee to forecast Chinook salmon returns to the Columbia River (*Mark Sorel*, *personal communication*) and the Fisheries Research Institute to forecast sockeye salmon returns to Bristol Bay (Ovando et al., 2022). Model averaging is a well-studied approach to predictive inference and is generally considered to be a useful tool in ecology where noisy data abound (Dormann et al., 2018). Finally, the proposed approach expands upon the simpler multi-model approach featuring weighted ensembles with one-step-ahead simulated retrospective forecasts to evaluate performance that was approved through the Council's methodology review process for use in forecasting Willapa Bay Coho in 2021 (Auerbach et al., 2021). We believe this is a robust approach that will improve OPI-H forecasts and has the potential to improve other stock unit forecasts.

Recommended Forecast Method

Preseason forecasts of salmon stocks are critical metrics for salmon fishery management and conservation. Our analysis has identified an ARIMA-based ensemble forecast approach that substantially reduced the forecast error compared to the current approach. Due to the MAPE weighted harmonic mean ensemble model resulting in the lowest one-step-ahead MAPE score over the 15 most recent years, and the benefits of ensemble forecasts, we recommend the MAPE weighted ensemble forecast methodology be adopted as the preferred method for forecasting total OPI-H pre-fishing adult ocean abundance.

While we found that weighting models based on the inverse of their MAPE using a simple harmonic mean led to better performance than other approaches, we recognize that it would be possible to select whichever ensemble or individual model performed bast in the most recent 15-years, even if the approach of calculating weights or selecting an individual model differed from year to year (e.g., a "best individual model or ensemble" approach). We did not evaluate the performance of this slightly different approach but could do so and report the results to the Council in a future report. We also have explored using machine learning approaches for individual and ensemble model construction, including ridge regression and gradient boosted random forests. These approaches did not out-perform ARIMA models and the simpler ensemble methods presented herein, and we consequently chose not to present these results. However, we intend to continue to explore these methods and others all within the same framework of out-of-sample performance evaluation described in this report with the goal of continuing to improve OPI-H Coho forecast performance.

The OPITT is confident in our ability to maintain and utilize the MAPE weighted ensemble forecasting model. Data inputs required for annual forecasting would remain the same for the jack returns and smolt release data. Environmental covariate data are easily accessed through public domains and the data are updated before the annual OPITT meeting where the forecast is produced. For transparency and reproducibility, the R code that produces the forecast is publicly posted on GitHub at https://github.com/wdfw-fp/OPI-H-Forecast-Evaluation-2023, and we plan to formulate it into an R package for ease of implementation.

Acknowledgments

We would like to acknowledge Erik Suring, ODFW Salmonid Life Cycle Monitoring, for sharing his knowledge of the current methodology and for his contributions to the historical OPI documentation that was greatly appreciated during this analysis. We would also like to thank Jon Carey, NOAA West Coast Region, for his support and knowledge of the current methodology and Council procedures.

References

Cheung, W.W., and Frölicher, T.L., 2020. Marine heatwaves exacerbate climate change impacts for fisheries in the northeast Pacific. Scientific reports, 10(1), p.6678.

Crozier, L.G., Burke, B.J., Chasco, B.E., Widener, D.L., and Zabel, R.W., 2021. Climate change threatens Chinook salmon throughout their life cycle. Communications Biology, 4(1), p.222.

Dormann, C.F., Calabrese, J.M., Guillera-Arroita, G., Matechou, E., Bahn, V., Bartoń, K., Beale, C.M., Ciuti, S., Elith, J., Gerstner, and K., Guelat, J., 2018. Model averaging in ecology: A review of Bayesian, information-theoretic, and tactical approaches for predictive inference. Ecological Monographs, 88(4), pp.485-504.

Hyndman, R., Athanasopoulos, G., Bergmeir, C., Caceres, G., Chhay L, O'Hara-Wild, M., Petropoulos, F., Razbash, S., Wang, E., and Yasmeen, F., 2023. forecast: Forecasting functions for time series and linear models. R package version 8.21.1, https://pkg.robjhyndman.com/forecast/.

Hyndman, R.J., and Khandakar, Y., 2008. Automatic time series forecasting: the forecast package for R. Journal of Statistical Software, 26(3), 1–22. doi:10.18637/jss.v027.i03.

Litzow, M.A., Hunsicker, M.E., Bond, N.A., Burke, B.J., Cunningham, C.J., Gosselin, J.L., Norton, E.L., Ward, E.J., and Zador, S.G., 2020. The changing physical and ecological meanings of North Pacific Ocean climate indices. Proceedings of the National Academy of Sciences, 117(14), pp.7665-7671.

NOAA (National Oceanic and Atmospheric Administration). 2021. Extended reconstructed sea surface temperature (ERSST.v5). National Centers for Environmental Information.

(Accessed February 2021). https://www.ncei.noaa.gov/products/extended-reconstructed-sst.

Ovando, D., Cunningham, C., Kuriyama, P., Boatright, C. and Hilborn, R., 2022. Improving forecasts of sockeye salmon (Oncorhynchus nerka) with parametric and nonparametric models. Canadian Journal of Fisheries and Aquatic Sciences, 79(8), pp.1198-1210.

Packer, J.F., Haymes, J.D., and Cook-Tabor, C., 2007. Coho FRAM Base Period Development. Pacific Fishery Management Council, 7700 NE Ambassador Place, Suite 101, Portland, Oregon 97220-1384.

PFMC (Pacific Fishery Management Council), 2023. Preseason Report I: Stock Abundance Analysis and Environmental Assessment Part 1 for 2023 Ocean Salmon Fishery Regulations. Pacific Fishery Management Council, 7700 NE Ambassador Place, Suite 101, Portland, Oregon 97220-1384. (Accessed September 2023).

Rupp, D.E., Wainwright, T.C., Lawson, P.W., and Peterson, W.T., 2012. Marine environment-based forecasting of coho salmon (*Oncorhynchus kisutch*) adult recruitment. Fisheries Oceanography, 21(1), pp.1-19.

Auerbach, D., Buehrens, T., Kendall, N., 2021. A proposed forecast methodology for natural-origin Willapa Bay Coho (*O. kisutch*). PFMC November 2021 Council Meeting Breifing Book. Agenda Item F.1, Attachment 3. Pacific Fishery Management Council, 7700 NE Ambassador Place, Suite 101, Portland, Oregon 97220-1384.

Smyth, P., and Wolpert, D., 1999. Linearly combining density estimators via stacking. Machine Learning, 36, pp.59-83.

Suring, E., and O'Farrell, M., 2021. Oregon Production Index Hatchery forecast methodology summary. PFMC November 2021 Council Meeting Breifing Book. Agenda Item F.1, Attachment 4. Pacific Fishery Management Council, 7700 NE Ambassador Place, Suite 101, Portland, Oregon 97220-1384.

Appendix

Table A1: One-year-ahead forecasted abundance of OPI Coho based on the MAPE-weighted ensemble approach compared to the actual abundance.

Year	Model	Abundance	Predicted abundance	Lo 50	Hi 50	Lo 95	Hi 95	error	% error
2008	MAPE_weighted	576.9	561.32	417.23	756.83	238.73	1344.60	-15.58	-0.03
2009	MAPE_weighted	1051.0	846.88	620.89	1155.14	343.64	2087.26	-204.12	-0.19
2010	MAPE_weighted	546.5	585.85	430.79	796.73	239.78	1431.50	39.35	0.07
2011	MAPE_weighted	454.2	786.87	576.24	1074.70	318.39	1947.77	332.67	0.73
2012	MAPE_weighted	183.1	385.01	317.92	466.30	220.78	671.97	201.91	1.10
2013	MAPE_weighted	335.1	563.29	461.57	687.45	315.80	1004.92	228.19	0.68
2014	MAPE_weighted	1316.5	1158.83	947.48	1417.35	645.52	2080.49	-157.67	-0.12
2015	MAPE_weighted	268.9	392.07	321.20	478.58	219.67	699.82	123.17	0.46
2016	MAPE_weighted	247.7	269.40	220.60	329.01	150.72	481.58	21.70	0.09
2017	MAPE_weighted	291.8	331.71	272.26	404.14	186.87	588.85	39.91	0.14
2018	MAPE_weighted	182.8	276.56	227.63	336.02	157.05	487.02	93.76	0.51
2019	MAPE_weighted	340.7	458.98	377.14	558.57	259.39	812.14	118.28	0.35
2020	MAPE_weighted	387.7	226.20	186.02	275.05	128.15	399.28	-161.50	-0.42
2021	MAPE_weighted	841.3	545.64	447.03	666.00	305.74	973.78	-295.66	-0.35
2022	MAPE_weighted	696.0	534.63	437.51	653.30	298.58	957.30	-161.37	-0.23
2023	MAPE_weighted	NA	484.00	396.36	591.02	270.86	864.89	NA	NA

Table A2. List of facilities that contribute to the jack escapement values used in the jack return covariate.

Reporting Agency [a/]	Area	Facility
WDFW	Columbia River	Beaver Creek Hatchery
ODFW	Columbia River	Big Creek Hatchery
FPC	Columbia River	Bonneville Dam
ODFW	Columbia River	Bonneville Hatchery
PGE	Columbia River	Clackamas Dam
ODFW	Columbia River	Clatsop County Fisheries
WDFW	Columbia River	Cowlitz Salmon Hatchery
USFWS	Columbia River	Eagle Creek National Fish Hatchery
WDFW	Columbia River	Fallert Creek Fish Hatchery
WDFW	Columbia River	Foster Road Trap (Elochoman River)
WDFW	Columbia River	Grays River Hatchery
WDFW	Columbia River	Kalama Falls Hatchery
ODFW	Columbia River	Klaskanine Hatchery
WDFW	Columbia River	Lewis River Hatchery
ODFW	Columbia River	Marmot Dam
WDFW	Columbia River	Merwin Dam (Lewis River)
WDFW	Columbia River	Modrow Trap (Kalama River)
WDFW	Columbia River	North Toutle Hatchery
ODFW	Columbia River	Sandy Hatchery
WDFW	Columbia River	Washougal Hatchery
WDFW	Columbia River	Washougal River Fish Weir
FPC	Columbia River	Willamette Falls
ODFW	OR/CA Coast	Bandon Hatchery
ODFW	OR/CA Coast	Cedar Creek Hatchery
ODFW	OR/CA Coast	Cole Rivers Hatchery
ODFW	OR/CA Coast	Eel Lake Hatchery
ODFW	OR/CA Coast	Elk River Hatchery
ODFW	OR/CA Coast	Fall Creek Hatchery
CDFW	OR/CA Coast	Iron Gate Fish Hatchery
ODFW	OR/CA Coast	Nehalem Hatchery
ODFW	OR/CA Coast	Newport Hatchery
ODFW	OR/CA Coast	Salmon River Hatchery
ODFW	OR/CA Coast	Trask Hatchery
CDFW	OR/CA Coast	Trinity River Hatchery

a/ CDFW, California Department of Fish and Wildlife; FPC, Fish Passage Center; ODFW, Oregon Department of Fish and Wildlife; PGE, Portland General Electric Company; USFWS, United States Fish and Wildlife Service; WDFW, Washington Department of Fish and Wildlife

Table A3. List of hatchery facilities that produce smolts whose release values are used in the smolt release covariate. Smolt release sites are not listed as they vary by year.

Reporting Agency [a/]	Area	Hatchery Rearing Facility
WDFW	Columbia River	Beaver Creek Hatchery
ODFW	Columbia River	Big Creek Hatchery
ODFW	Columbia River	Bonneville Hatchery
YAKA	Columbia River	Cascade Hatchery
ODFW	Columbia River	Clatsop County Fisheries
WDFW	Columbia River	Cowlitz Salmon Hatchery
WDFW	Columbia River	Deep River Net Pens
USFWS	Columbia River	Dworshak National Hatchery
USFWS	Columbia River	Eagle Creek National Fish Hatchery
WDFW	Columbia River	Grays River Hatchery
WDFW	Columbia River	Kalama Falls Hatchery
ODFW	Columbia River	Klaskanine Hatchery
YAKA	Columbia River	Klickitat Hatchery
USFWS	Columbia River	Leavenworth Hatchery
WDFW	Columbia River	Lewis River Hatchery
WDFW	Columbia River	North Toutle Hatchery
YAKA	Columbia River	Prosser Hatchery
ODFW	Columbia River	Sandy Hatchery
WDFW	Columbia River	Washougal Hatchery
DPUD	Columbia River	Wells Fish Hatchery
YAKA	Columbia River	Willard National Fish Hatchery
YAKA	Columbia River	Winthrop National Fish Hatchery
ODFW	OR/CA Coast	Cole Rivers Hatchery
CDFW	OR/CA Coast	Iron Gate Fish Hatchery
ODFW	OR/CA Coast	Nehalem Hatchery
ODFW	OR/CA Coast	Rock Creek Hatchery
ODFW	OR/CA Coast	Trask Hatchery
CDFW	OR/CA Coast	Trinity River Hatchery

a/ CDFW, California Department of Fish and Wildlife; DPUD, Douglas County Public Utility District; ODFW, Oregon Department of Fish and Wildlife; USFWS, United States Fish and Wildlife Service; WDFW, Washington Department of Fish and Wildlife; YAKA, Yakama Nation

Table A4. OPI-H Coho postseason MSM abundance estimate (thousands; “abundance”) and covariates used in models.

year	species	abundance	lag1_log_JackOPI	lag1_log_SmAdj	lag1_NPGO	lag1_PDO	WSST_A	PDO.MJJ	MEI.OND	UWI.JAS	SST.AMJ	SSH.AMJ	UWI.SON
1970	Coho	2765.1	5.09	0.00	-0.39	0.00	0.21	-0.25	0.36	34.70	11.97	-38.47	-34.01
1971	Coho	3365.0	5.19	0.00	0.06	-0.12	-0.80	-0.33	-1.30	41.41	10.88	-153.03	-31.81
1972	Coho	1924.8	4.64	0.00	0.38	-0.97	-1.14	-0.50	-1.59	28.96	11.69	-71.83	-16.05
1973	Coho	1817.0	4.52	0.27	-0.66	-0.76	-1.05	-0.82	1.44	33.79	11.85	-64.73	-8.15
1974	Coho	3071.1	4.97	0.50	0.13	-0.65	-0.76	-1.08	-1.80	41.15	12.24	-157.53	-19.50
1975	Coho	1652.8	4.33	0.28	-0.01	-0.07	-0.20	-1.04	-1.37	33.20	10.94	-77.83	-8.79
1976	Coho	3885.3	5.14	0.34	0.80	-0.94	-0.63	-0.82	-2.10	38.46	10.83	-154.43	-38.99
1977	Coho	987.5	3.99	0.03	1.86	0.01	0.52	-0.52	0.50	22.62	10.69	-116.00	-7.94
1978	Coho	1824.1	4.64	0.00	1.25	0.33	-0.10	-0.26	0.74	30.15	11.20	-139.73	-34.77
1979	Coho	1476.7	4.28	0.64	0.50	0.38	-0.55	-0.22	-0.15	16.88	11.58	-90.37	-5.59
1980	Coho	1224.0	4.05	0.91	-0.74	0.44	0.65	0.17	0.38	24.02	11.22	-94.83	-58.73
1981	Coho	1064.5	3.89	0.74	-0.75	0.56	0.15	0.34	0.03	48.08	12.06	-67.03	-42.72
1982	Coho	1266.8	4.12	0.84	-0.22	0.99	-0.13	0.62	-0.16	28.80	12.15	-84.00	-54.10
1983	Coho	NA	4.22	0.74	-0.69	0.09	0.07	0.57	2.10	28.85	10.98	-70.73	-42.97
1984	Coho	691.3	3.45	0.63	-0.09	1.23	0.22	1.03	-0.43	26.44	12.14	-6.43	-46.62
1985	Coho	717.5	3.26	0.90	0.62	0.71	-0.26	1.04	-0.36	38.12	11.43	-64.20	-52.44
1986	Coho	2412.0	4.35	1.77	-0.39	0.32	-1.12	0.79	-0.02	36.91	10.95	-80.83	-12.17
1987	Coho	779.4	3.49	0.87	-0.73	1.20	-0.08	1.14	0.61	38.46	11.51	-81.87	-19.72
1988	Coho	1467.8	4.45	1.14	0.43	1.36	0.29	0.88	0.99	36.07	11.43	-79.57	-34.08
1989	Coho	1922.0	4.11	0.98	1.32	0.19	-0.32	0.99	-1.57	42.69	11.49	-61.47	-20.23
1990	Coho	713.6	3.84	1.04	0.61	-0.29	0.12	1.02	-0.44	35.53	11.62	-63.43	-4.82
1991	Coho	1816.5	4.23	0.96	-0.20	-0.48	-0.62	0.83	0.03	42.94	12.01	-61.60	-12.08
1992	Coho	512.6	3.24	0.51	-0.50	-0.54	-0.11	0.28	1.13	39.48	10.92	-107.47	-2.08
1993	Coho	223.3	3.30	0.50	-1.09	0.89	0.08	0.45	0.77	36.75	12.72	-26.77	-24.99
1994	Coho	214.1	1.65	0.24	-1.90	1.17	0.12	0.88	0.82	40.86	13.24	63.40	0.14
1995	Coho	139.4	2.47	0.26	-1.21	-0.18	0.08	0.93	1.23	39.04	11.45	-59.57	-13.29
1996	Coho	176.5	2.85	0.44	-1.04	0.63	0.66	1.48	-0.66	27.53	11.19	-59.37	-25.28
1997	Coho	195.6	3.02	0.34	-0.97	0.81	0.06	1.42	-0.30	56.80	11.44	-41.63	-4.70
1998	Coho	228.3	2.27	0.23	-0.66	1.34	1.48	1.43	2.04	10.18	12.10	-8.30	-55.94
1999	Coho	372.5	3.38	0.35	0.54	-0.12	0.47	1.37	-1.25	49.68	11.38	-34.40	-43.26
2000	Coho	673.1	3.55	0.51	1.52	-1.38	-0.21	0.78	-1.32	51.00	10.67	-103.47	-34.18
2001	Coho	1478.7	4.47	0.28	1.89	-0.78	0.09	0.35	-0.73	35.78	11.36	-46.77	-26.83
2002	Coho	689.5	3.23	0.16	2.08	-0.74	-0.28	-0.40	-0.28	47.08	10.68	-116.13	-38.19
2003	Coho	1009.9	3.91	0.05	1.47	-0.13	0.31	-0.60	0.78	50.48	10.11	-137.93	-25.90
2004	Coho	693.6	3.57	0.29	0.96	0.53	0.28	-0.17	0.28	55.48	11.08	-52.07	-26.35
2005	Coho	454.0	3.22	0.11	0.21	-0.11	-0.06	0.04	0.42	26.99	11.86	-50.60	4.34
2006	Coho	523.4	3.25	0.06	-1.47	-0.09	0.37	0.52	-0.73	51.75	12.54	-13.00	-9.01
2007	Coho	545.3	3.59	0.02	-0.55	-0.15	-0.24	0.79	0.79	53.57	11.15	-23.07	-14.10
2008	Coho	576.9	2.78	0.08	0.58	-0.46	-0.62	0.64	-1.14	27.52	10.62	-109.77	-9.88
2009	Coho	1051.0	4.10	0.20	1.49	-1.33	-0.77	0.16	-1.08	32.71	9.62	-98.67	-10.66
2010	Coho	546.5	3.23	0.03	0.64	-0.82	-0.26	-0.29	0.80	24.32	10.45	-80.77	-47.08
2011	Coho	454.2	3.15	0.05	1.29	-0.74	0.11	-0.50	-2.11	34.21	11.68	-32.63	-32.89
2012	Coho	183.1	2.88	0.12	0.79	-1.57	-0.09	-0.81	-1.29	29.33	10.70	-29.73	-26.30
2013	Coho	335.1	3.27	0.19	1.42	-1.41	-0.05	-0.74	-0.14	53.55	11.02	-17.30	-29.90
2014	Coho	1316.5	3.94	0.13	0.36	-0.93	-0.38	-0.76	-0.17	35.30	10.66	-88.80	-7.81
2015	Coho	268.9	3.68	0.29	-0.20	0.53	1.59	-0.43	0.20	41.26	11.17	-11.57	-40.11
2016	Coho	247.7	2.98	0.21	-1.38	0.80	0.92	0.19	2.00	40.41	10.28	-97.97	-7.85
2017	Coho	291.8	3.13	0.23	-0.16	0.63	0.86	0.97	-0.56	47.98	11.58	-108.50	-68.23
2018	Coho	182.8	2.95	0.12	-0.86	-0.06	0.41	1.28	-0.63	46.09	11.19	-49.77	-36.18
2019	Coho	340.7	3.86	0.10	-1.96	-0.30	0.73	1.01	0.34	41.06	10.82	-104.60	-12.37
2020	Coho	387.7	2.72	0.03	-2.28	-0.03	-0.08	0.89	0.36	20.07	10.47	-86.57	4.07
2021	Coho	841.3	4.53	0.10	-1.84	-1.04	0.47	0.39	-1.18	25.56	11.40	-71.27	-18.89
2022	Coho	696.0	4.15	0.07	-0.91	-1.57	-0.13	-0.09	-1.44	40.84	10.97	-123.17	-64.07
2023	Coho	NA	3.97	0.07	-1.31	-1.77	-0.04	-0.60	-1.64	33.83	11.47	-90.30	-6.61